Understanding Quantum Synchronization of Self-Sustained Oscillators through Coherence

A Thesis

submitted to
Indian Institute of Science Education and Research Pune
in partial fulfillment of the requirements for the
BS-MS Dual Degree Programme

by

Mohit Kumar

Indian Institute of Science Education and Research Pune
Dr. Homi Bhabha Road,
Pashan, Pune 411008, INDIA.

May, 2025

Supervisor: Dr. Bijay Kumar Agarwalla

Certificate

This is to certify that this dissertation entitled Understanding Quantum Synchronization of Self-Sustained Oscillators through Coherencetowards the partial fulfilment of the BS-MS dual degree programme at the Indian Institute of Science Education and Research, Pune represents study/work carried out by Mohit Kumar at Indian Institute of Science Education and Research under the supervision of Dr. Bijay Kumar Agarwalla, Associate Professor, Department of Physics , during the academic year 2020-2025.

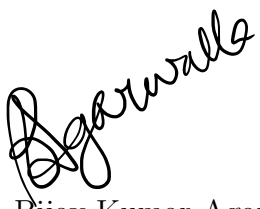

Dr. Bijay Kumar Agarwalla

Committee:

Dr. Bijay Kumar Agarwalla

Prof. T.S. Mahesh

This thesis is dedicated to my friends and family.

Declaration

I hereby declare that the matter embodied in the report entitled Understanding Quantum Synchronization of Self-Sustained Oscillators through Coherence are the results of the work carried out by me at the Department of Physics, Indian Institute of Science Education and Research, Pune, under the supervision of Dr. Bijay Kumar Agarwalla and the same has not been submitted elsewhere for any other degree.

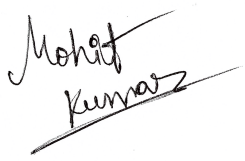

Mohit Kumar

Acknowledgments

I would like to express my deepest gratitude to my advisor, Dr. Bijay Kumar Agarwalla, for his invaluable guidance, support, and encouragement throughout this research journey. His expertise has been crucial in shaping this work, and I am truly grateful for his patience and mentorship. I would also like to extend my sincere thanks to Prof. T.S. Mahesh, who introduced me to the field of quantum synchronization. His valuable insights and suggestions have significantly contributed to the progress of this project. I am deeply grateful to my family for their unwavering support, patience, and encouragement throughout my academic journey. Their belief in me has been a constant source of motivation.

This thesis would not have been possible without the collective support of all these individuals, and I sincerely thank each one of them.

Abstract

Quantum synchronization, the emergence of phase locking in quantum systems, has gained significant attention due to its potential applications in quantum technologies. In this thesis, we analytically investigate the resources responsible for synchronization in various setups and the generation of these resources via different forms of interactions and drives. We further investigate the connection of coherences and correlations to the synchronization of various systems. We further dive into many examples and counter examples to show that there is no one-to-one correspondence between synchronization and the existence of coherence, correlations, or entanglement.

As model examples we study synchronization in infinite dimensional systems with a clear classical analog, like a quantum harmonic oscillator, and in purely quantum mechanical finite-dimensional spin systems. We use the Lindblad formalism to model self-sustained oscillators with a free phase in continuous variable and discrete variable systems and we use tools from quantum optics like phase space representations and coherent states to quantify synchronization.

Our findings show how specific coherences are the deciding factor for synchronization and how their existence still doesn't guarantee synchronization due to the possibility of destructive interference.

Contents

List of Figures

Chapter 1

Introduction

Synchronization is a fundamental phenomenon that manifests across a diverse range of physical, chemical, and biological systems [1]. It governs processes from the coordinated flashing of fireflies to the collective motion of coupled oscillators such as metronomes. The term "synchronization" originates from the Greek words 'syn-' meaning "together with" and 'kronous' meaning "time," indicating the occurrence of events in unison. Formally, synchronization describes a scenario where the dynamics of two or more systems become correlated in frequency or phase due to their interaction.

The scientific study of synchronization can be traced back to 1673 when Christian Huygens observed an intriguing effect in pendulum clocks. He noticed that two pendula, when weakly coupled through a common support, would eventually synchronize their oscillations in phase and frequency. This discovery laid the foundation for the study of synchronized dynamical systems. Since then, synchronization has been extensively studied in classical systems [2, 3], encompassing areas such as nonlinear dynamics, neuroscience, electrical circuits, and even large-scale phenomena like climate oscillations.

While classical synchronization is well understood, the study of synchronization in quantum systems has garnered significant attention in recent years [4, 5]. Unlike classical oscillators, these systems exhibit fundamental differences due to quantum principles like superposition and entanglement. Quantum synchronization refers to the emergence of correlated dynamics in quantum oscillators, often studied in open quantum systems where dissipation and external driving play crucial roles. Research in this area explores how quantum effects

influence synchronization and whether classical synchronization concepts can be extended to the quantum domain.

Synchronization could be defined as the mutual adjustment of rhythms of two bodies due to an interaction [1]. A general approach to synchronization studies is as follows:

1. First we model a Self-Sustained Oscillator (SSO) capable of maintaining oscillations without any external forcing, this is possible due to the presence of time-independent gain and loss terms. The SSO has a limit-cycle behavior, which means that given any initial state, the oscillator always relaxes to the same steady-state trajectory.

2. The setup consists of an SSO or a collection of SSO, this setup must have a free phase variable ϕ. This means that without the introduction of any drive or coupling in the system, it must be non-selective of any phase, which implies that if we plot the probability distribution $P(\phi)$ over the phase variable ϕ, we receive a uniform distribution of $1/2\pi$.

3. When we introduce an external drive or coupling of appropriate form in the setup, the system starts to become selective in its phase ϕ. This means that $P(\phi)$ would have a non-uniform distribution and this is called synchronization.

Quantum synchronization has been explored in a wide range of setups, involving different types of oscillators, various driving mechanisms, and multiple forms of coupling. Despite the diversity of these studies, they generally follow the three-step approach described above, yet the results vary across different systems. In this work, we aim to bridge the gap between these studies by identifying a unifying principle underlying all forms of quantum synchronization. To achieve this, we analytically examine the phase space of oscillators. Our approach focuses on identifying the fundamental resource responsible for synchronization, understanding its role in different setups, and establishing a coherent framework that connects seemingly distinct synchronization mechanisms. Furthermore, we investigate how these synchronization-enabling resources can be generated within a system and analyze the factors that lead to their degradation or destruction. By uncovering these fundamental aspects, our study provides a deeper understanding of quantum synchronization and offers insights into optimizing its presence in practical quantum systems.

The thesis is organized as follows, in Chapter 2 we study the synchronization of a continuous variable non-linear oscillator to an external drive, in Chapter 3 we study the synchronization between two continuous variable non-linear oscillators and how they influence each other's phase. In Chapter 4 we extend our study to synchronization of a purely quantum mechanical finite-dimensional spin system to an external drive and in Chapter 5 we study synchronization between two such spin systems.

Chapter 2

Synchronization of a Harmonic Oscillator to a Drive

Synchronization in classical systems is typically studied using continuous-variable setups, such as harmonic oscillators. The quantum harmonic oscillator serves as the most natural counterpart for investigating synchronization in the quantum regime, as it retains key features of classical systems while incorporating inherently quantum properties, such as the uncertainty principle. In this chapter, we establish a framework for studying quantum synchronization in infinite-dimensional systems.

The chapter is organized as follows, in sec 2.1 we review a classical model for the self-sustained oscillator, i.e. a Van der Pol oscillator. In sec 2.2 we model a quantum analog for the Van der Pol oscillator by supplying appropriate gain and loss to a quantum harmonic oscillator. In sec 2.3 we derive an analytical formula to plot the phase distribution for a harmonic oscillator and finally in sec 2.4 we drive the quantum oscillator and study its synchronization properties.

2.1 Classical VdP

The study of classical synchronization uses a continuous variable (CV) system like a harmonic oscillator, when it is supplied with additional gain and loss terms we obtain an SSO. The

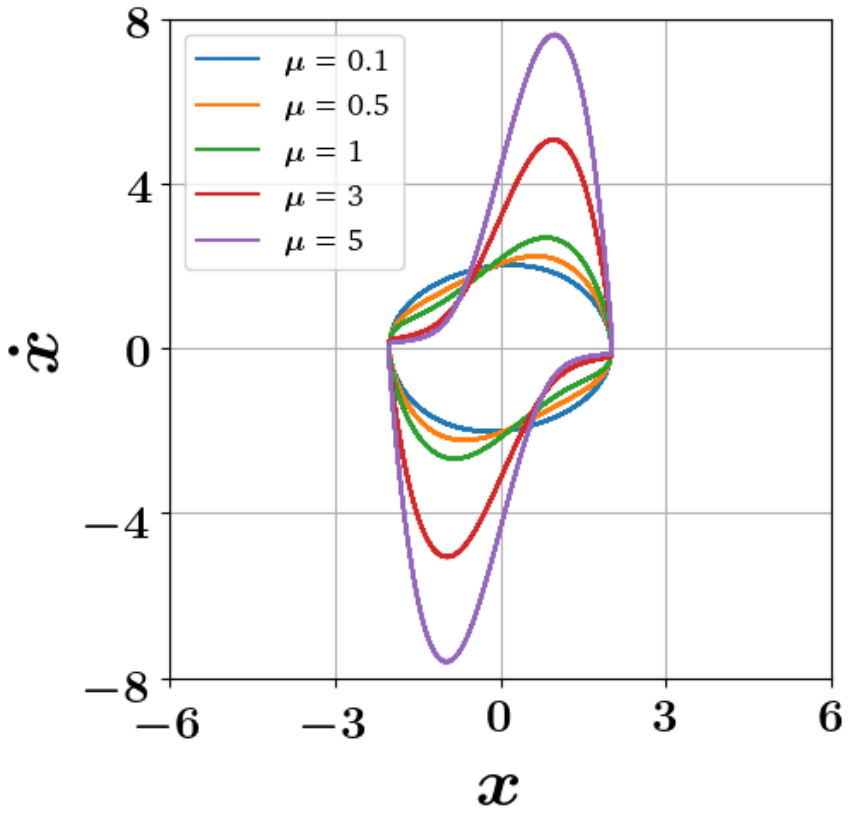

Figure 2.1: Steady-state limit cycle for VdP (Eq 2.2) with different nonlinearities μ and $\omega_0 = 1$. As we can see, for small μ the limit cycle is similar to the trajectory of a harmonic oscillator with small deformation, as μ increases the deformation increases.

general form for such an oscillator could be given by

$$\ddot{x} + \omega_0^2 x = f(x, \dot{x}), \tag{2.1}$$

where ω_0 is the natural oscillator and $f(x, \dot{x})$ is the supplied gain and loss terms. The limit cycle behavior of an SSO needs a balance between the loss and gain processes such that the oscillator is stabilized at a non-zero amplitude. This requires the introduction of nonlinearity in the system to prevent the oscillator from going to the ground state. The most widely used model of SSO is the Van der Pol (VdP) oscillator [6], it is the workhorse of synchronization studies, and it is modeled by supplying a linear gain and non-linear loss to a harmonic oscillator. It has been used to study electrical circuits to circadian rhythms

[7, 8]. The EOM for a VdP is given by

$$\ddot{x} + \omega_0^2 x = \mu(1 - x^2)\dot{x}, \tag{2.2}$$

here μ is the strength of non-linearity in the system. For small μ VdP has a limit cycle similar to the trajectory of a harmonic oscillator, as non-linearity increases the trajectory is deformed. As we could see from the Eq 2.2, the non-linear term $(1 - x^2)$ is negative for large x which leads to a damping effect, and the system is stabilized back to the limit cycle, similarly for small x the term becomes negative which leads to pumping and oscillator regains its stable amplitude. This is how the limit-cycle behavior is achieved for a VdP. Moreover, as we could see from the EOM of VdP, there are no time-dependent terms in the equation, this removes any time reference for the oscillator leading to a free phase. The information about phase ϕ is derived from the phase space trajectory in the steady state. For a single oscillator, a 2-dimensional phase space is formed by $(x, \dot{x})$, similarly for n oscillators we have a 2^n-dimensional phase space. To extract the phase information, we transform the phase space distribution from Cartesian coordinates to polar coordinates and integrate out all the variables other than ϕ.

2.2 Quantum VdP

To study synchronization in the quantum domain the first thing we require is a quantum SSO. As we saw in sec 2.1, to model such an oscillator we require a balance between linear gain and non-linear loss processes. To mimic a classical VdP in the quantum regime, we use Lindblad dissipators to supply incoherent gain and loss to a Quantum Harmonic Oscillator (QHO). A Quantum Van der Pol (QVdP) oscillator [9] is defined by the following Lindblad master equation

$$\dot{\tilde{\rho}} = -i\left[\omega_0 a^\dagger a, \tilde{\rho}\right] + \gamma_g \mathcal{D}[a^\dagger]\tilde{\rho} + \gamma_l \mathcal{D}[a^2]\tilde{\rho}, \tag{2.3}$$

with γ_g and γ_l being the gain and loss rates for the QVdP and ω_0 is the natural frequency of the oscillator. Here a and $a^\dagger$ are the standard annihilation and creation operators, and $\mathcal{D}$ are the Lindbladian dissipators, $\mathcal{D}[O]\tilde{\rho} = O\tilde{\rho}O^\dagger - \frac{1}{2}\{O^\dagger O, \tilde{\rho}\}$.

Eq 2.3 gives a steady state that is diagonal in the Fock basis with no coherences [9]. The

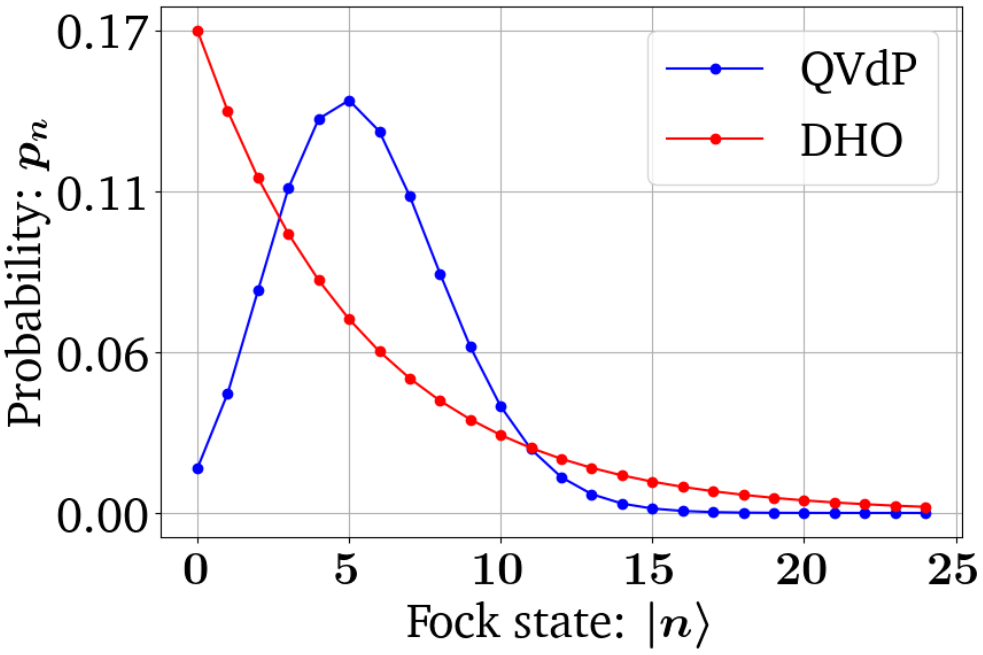

Figure 2.2: Fock state distribution, given by $\langle n|\,\rho\,|n\rangle$, for the steady-state density matrices of a Quantum Van der Pol oscillator (QVdP) with $\gamma_l = 0.1$ and $\gamma_g = 1$, and a Damped Harmonic Oscillator (DHO) with $\gamma_l = 1.2$ and $\gamma_g = 1$. Both have the natural frequency $\omega_0 = 1$. We could see that unlike a thermal state, the steady state of a QVdP has the highest occupation probability above the ground state and can be controlled by varying $\beta = \gamma_l/\gamma_g$.

steady state is of the form

$$\tilde{\rho}_{ss} = \sum_{n=0}^{\infty} p_n \,|n\rangle\,\langle n|\,. \tag{2.4}$$

As we can see, ρ_{ss} is in the statistical superposition of Fock states, very similar to the steady state of a damped harmonic oscillator (DHO), i.e. a thermal state. Moreover, the master equation for a DHO is also similar to Eq 2.3, the only difference is that the loss is also linear in this case. The explicit master equation is given by

$$\dot{\tilde{\rho}} = -i\left[\omega_0 a^\dagger a, \tilde{\rho}\right] + \gamma_g \mathcal{D}[a^\dagger]\tilde{\rho} + \gamma_l \mathcal{D}[a]\tilde{\rho}\,. \tag{2.5}$$

The difference between the steady state of a DHO and a QVdP is that in the former case, the Fock state with the highest probability of occupation is always $|0\rangle$, whereas in the latter case, it is $|n\rangle$ and n can be controlled by varying the loss and gain rates.

To isolate the effects of the dissipator on the evolution of the system, we go into the frame rotating with natural frequency ω_0. The new density matrix in this frame is given by

$$\rho = \exp\left(i\omega_0 a^\dagger a\right)\tilde{\rho}\exp\left(-i\omega_0 a^\dagger a\right) \ . \tag{2.6}$$

The master equation in the rotating frame is given by

$$\dot{\rho} = \gamma_1 \mathcal{D}[a^\dagger]\rho + \gamma_2 \mathcal{D}[a^2]\rho \ . \tag{2.7}$$

The mean field equation for evolution of complex amplitude $\alpha = \langle a \rangle$ in the classical limit of $\langle a^\dagger a \rangle >> 1$ is given by [10]

$$\dot{\alpha} = \frac{\gamma_g}{2}\ \alpha - \gamma_l\ \alpha|\alpha^2| \ . \tag{2.8}$$

For the steady state with $\dot{\alpha} = 0$, the system settles to a fixed amplitude of $|\alpha| = \gamma_g/2\gamma_l$. In the mean-field limit $|\alpha|$ is equivalent to $\langle n \rangle$, thus the ratio of gain to loss rate determines the steady state average occupation of the QVdP. We define: $\beta = \gamma_l/\gamma_g$, this quantity is directly related to the average occupation of the QVdP and controls the quantum nature of the system. For large β the system comes closer to the ground state and quantum effects dominate.

For the case of a quantum oscillator, unlike its classical counterpart, we don't have an exact phase space representation. This is because due to the uncertainty principle, the state of the system cannot be defined by a single point in the phase space. To work around this problem we use quasiprobability phase space distributions [11]. We use a Wigner distribution to study the phase space properties of the QVdP. For a density matrix ρ, the Wigner distribution is defined as

$$W(x,p) = \frac{1}{\pi}\int_{-\infty}^{\infty} dy\ \langle x-y|\rho|x+y\rangle\ \exp(2ipy) \ . \tag{2.9}$$

The shape of the Wigner distribution for the steady state of a QVdP is an annular ring. The radial spread in the distribution is the result of quantum noise introduced due to the dissipators [10]. As we could see from fig 2.3, the steady state Wigner function is symmetrically distributed about the origin, thus we could say that similar to a VdP, a QVdP also possesses a free phase which could be utilized to study synchronization with a drive or between a collection of such oscillators.

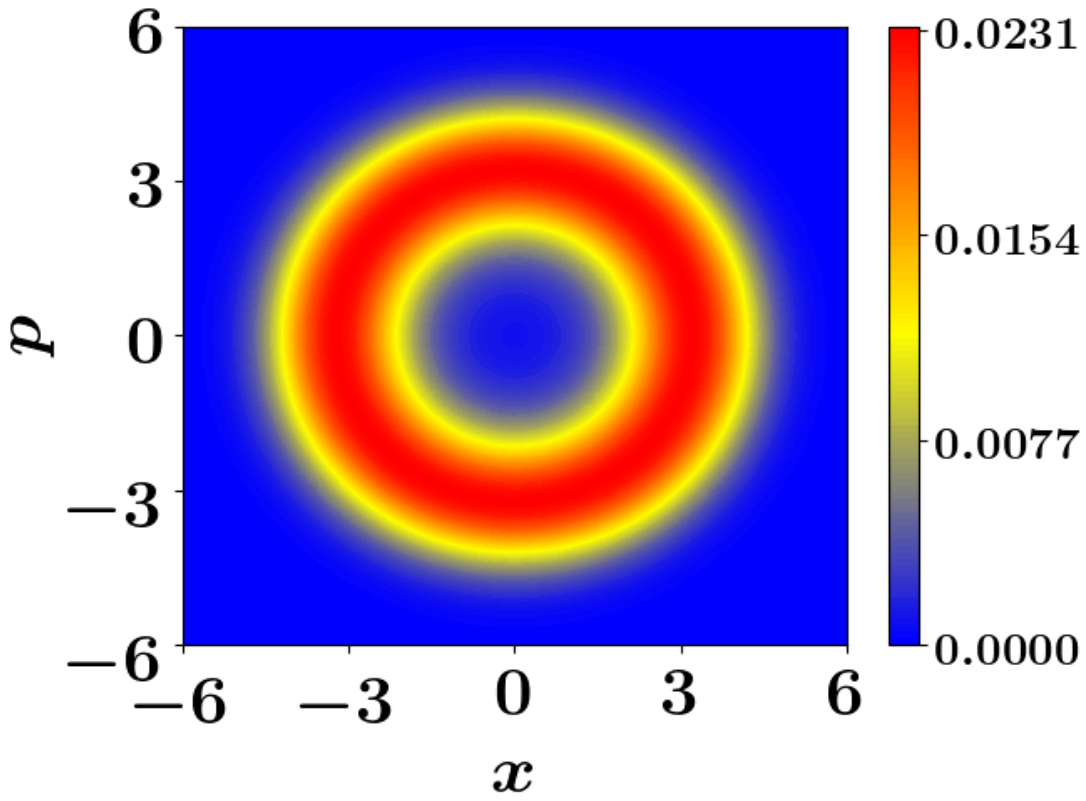

Figure 2.3: Wigner distribution for the steady state density matrix of QVdP with $\gamma_l = 0.1, \gamma_g = 1$ and $\omega_0 = 1$. This shape is similar to the classical circular limit cycle along with a spread due to quantum noise. Moreover, the circularly symmetric shape of the Wigner function tells us that it possesses a free phase and is non-selective on any phase angle.

As expected intuitively, if we keep increasing the loss-to-gain ratio β, the average occupation will go lower. Let $P(n,t) = \langle n|\rho(t)|n\rangle$, i.e. the probability of occupation of Fock state $|n\rangle$ at time t. The Pauli Master Equation [12] for the QVdP is given by

$$\dot{P}(n,t) = \gamma_g[nP(n-1,t)-(n+1)P(n,t)]+\gamma_l[(n+1)(n+2)P(n+2,t)-n(n-1)P(n,t)]\,. \quad (2.10)$$

The terms are due to one photon gain, one photon loss, two-photon gain, and two-photon loss, respectively. If we keep increasing the non-linear dissipation rate γ_2, the oscillator will go closer and closer to its ground state, in this process the discrete nature and quantum noise become prominent. If we take $\beta \to \infty$, the oscillator is said to be in the dissipative limit. In this case, the state of the oscillator will be close to the ground state, but due to our choice of non-linear loss and linear gain, the limit cycle still survives. For the dissipative limit only

the lowest two Fock states, $|0\rangle$ and $|1\rangle$ are occupied [9, 10] as the system has a two-photon loss which doesn't affect $|1\rangle$. The transition rates between the lowest three levels is given by:

$$|0\rangle \xrightarrow{\gamma_g} |1\rangle \xrightarrow{2\gamma_g} |2\rangle \xrightarrow{2\gamma_l} |0\rangle$$

As we are in the dissipative limit with $\gamma_2/\gamma_1 \to \infty$, the transition reduces to:

$$|0\rangle \xrightarrow{\gamma_g} |1\rangle \xrightarrow{2\gamma_g} |0\rangle$$

We could see that the QVdP spends twice as much time in the state $|0\rangle$, compared to $|1\rangle$, the steady state population of $|0\rangle$ would be twice compared to $|1\rangle$. ρ_{ss} in the dissipative limit is given by:

$$\rho_{ss} = \frac{2}{3}|0\rangle\langle 0| + \frac{1}{3}|1\rangle\langle 1| \tag{2.11}$$

2.3 Phase Distribution for a QHO

The information about the phase of a QHO state is embedded in its quasiprobability phase space distributions. As we saw in Eq 2.9 the Wigner distribution is defined over the phase space (x, p). Expanding the density matrix of the equation in the Fock basis we get

$$\begin{aligned} W(x,p) &= \frac{1}{\pi}\int_{-\infty}^{\infty} dy\ \langle x-y|\rho_{ss}|x+y\rangle\ \exp(2ipy) \\ &= \sum_{mn} \langle m|\,\rho\,|n\rangle\ \left[\frac{1}{\pi}\int_{-\infty}^{\infty} dy\ \langle x-y\,|m\rangle\,\langle n|\,x+y\rangle\ \exp(2ipy)\right] \\ &= \sum_{mn} \langle m|\,\rho\,|n\rangle\ W_{mn}(x,p)\ , \end{aligned} \tag{2.12}$$

where W_{mn} is the Wigner distribution for $|m\rangle\langle n|$ [13] given by

$$W_{mn}(x,p) = \sqrt{\frac{n!}{m!}} e^{i(n-m)\arctan(p/x)} \frac{(-1)^n}{\pi} \left(2(x^2+p^2)\right)^{(m-n)/2} L_n^{m-n}\left(2(x^2+p^2)\right) e^{-(x^2+p^2)}\ , \tag{2.13}$$

where L_n^{m-n} is the generalized Laguerre polynomial. To find the angular distribution we do a variable transform to polar coordinates (r, ϕ), where we define

$$r = \sqrt{x^2+p^2}\ ;\ \phi = \arctan\left(\frac{p}{x}\right) \bmod 2\pi\ . \tag{2.14}$$

After the transformation, we receive a Wigner distribution of the form $W(r,\phi)$. This is a joint probability distribution in r and ϕ, to obtain the marginal probability distribution $P(\phi)$ which is the phase distribution, we integrate out r with a proper Jacobian as follows

$$\begin{aligned} P_w(\phi) &= \int_0^\infty dr\ r\ W(r,\phi) \\ &= \sum_{mn} \langle m|\,\rho\,|n\rangle \int_0^\infty dr\ r\ W_{mn}(r,\phi)\ . \end{aligned} \tag{2.15}$$

In the polar coordinates W_{mn} could be written as

$$W_{mn}(r,\phi) = \sqrt{\frac{n!}{m!}} e^{i(n-m)\phi} \frac{(-1)^n}{\pi} \left(2r^2\right)^{(m-n)/2} L_n^{m-n}\left(2r^2\right) e^{-r^2}\ , \tag{2.16}$$

using this form of W_{mn}, $P_w(\phi)$ could be written as

$$\begin{aligned} P_w(\phi) &= \frac{1}{2\pi} \sum_{mn} \langle m|\rho|n\rangle\ R_w(m,n)\ \exp\{i(n-m)\phi\} \\ &= \frac{1}{2\pi} + \frac{1}{2\pi} \sum_{m\neq n} \langle m|\rho|n\rangle R_w(m,n)\ \exp\{i(n-m)\phi\}, \end{aligned} \tag{2.17}$$

where $R_w(m,n)$ is the integral of the radial part for the Wigner distribution, its explicit form is given by

$$R_w(m,n) = 2(-1)^n \sqrt{\frac{n!}{m!}} \int_0^\infty dr\ r \left(\sqrt{2}r\right)^{(m-n)} L_n^{m-n}(2r^2)\ e^{-r^2}\ , \tag{2.18}$$

with properties $R_w(m,m) = 1$ and $R_w(m,n) = R_w(n,m)$. As we could see from Eq 2.17, a density matrix state that is diagonal and has no coherence in the Fock basis produces a uniform $P_w(\phi)$ with value $1/2\pi$. This shows that all diagonal states have a free phase. For phase selectivity to exist, i.e. for $P_w(\phi)$ to be non-uniform, we require the existence of coherences $\langle m|\,\rho\,|n\rangle$. This shows that coherences between energy eigenstates act as a resource for the synchronization of a single oscillator [].

We define a new term C_k^w as follows

$$C_k^w = \sum_{m-n=k} \langle m|\,\rho\,|n\rangle\, R_w(m,n), \tag{2.19}$$

it could be decomposed into its angular and radial part as $C_k^w = A_k^w \exp(i\Theta_w^k)$. Using these definitions, the equation for $P_w(\phi)$ could be simplified as

$$\begin{aligned}
P_w(\phi) &= \frac{1}{2\pi} + \frac{1}{2\pi}\sum_{m\neq n}\langle m|\rho|n\rangle R_w(m,n)\ \exp\{i(n-m)\phi\} \\
&= \frac{1}{2\pi} + \frac{1}{2\pi}\sum_{m>n}\langle m|\rho|n\rangle R_w(m,n)\ \exp\{i(n-m)\phi\} + \langle n|\rho|m\rangle R_w(n,m)\ \exp\{i(m-n)\phi\} \\
&= \frac{1}{2\pi} + \frac{1}{2\pi}\sum_{k=1}^{\infty}\left[\exp(-ik\phi)\sum_{m-n=k}\langle m|\,\rho\,|n\rangle\, R_w(m,n)\right] + h.c. \\
&= \frac{1}{2\pi} + \frac{1}{2\pi}\sum_{k=1}^{\infty}[C_k^w\exp(-ik\phi)] + h.c. \\
&= \frac{1}{2\pi} + \frac{1}{2\pi}\sum_{k=1}^{\infty}[A_k^w\exp\{-i(k\phi-\Theta_k^w)\}] + h.c. \\
&= \frac{1}{2\pi} + \frac{1}{\pi}\sum_{k=1}^{\infty}A_k^w\cos(k\phi-\Theta_k^w)\ . \qquad (2.20)
\end{aligned}$$

This form of $P(\phi)$ tells us that the phase distribution could be written as a superposition of different harmonics. Let all the coherences $\langle m|\,\rho\,|n\rangle$ of the density matrix for a QHO form a set S, this set could be further divided into subsets $\{S_k\}$ based on the form $\langle m+k|\,\rho\,|m\rangle$. The elements of the subset S_k contribute to the k-th harmonic of $P(\phi)$ which leads to a distribution with k peaks between 0 to 2π. Let the subset with the largest A_k^w be S_{k_d}, this is the dominant subset because due to its contribution k_d is the dominant harmonic in $P(\phi)$ and will lead to k_d peaks. The position of peaks is given by $\phi_P = (\Theta_k + 2n\pi)/k_d$, where n is an integer.

Similar to the case of a Wigner function, we could also use a different quasi-probability distribution to find $P(\phi)$, for example, the Huisimi-Q distribution. The Q-function [14] for a harmonic oscillator with a state ρ is defined as:

$$Q(\alpha) = \frac{1}{\pi}\langle\alpha|\,\rho\,|\alpha\rangle \qquad (2.21)$$

where $|\alpha\rangle$ is the harmonic oscillator coherent state defined as:$|\alpha\rangle = e^{-\frac{|\alpha|^2}{2}}\sum_{n=0}^{\infty}\frac{\alpha^n}{\sqrt{n!}}|n\rangle$.

Expanding the equation for Q in terms of density matrix elements we get

$$\begin{aligned} Q(\alpha) &= \frac{1}{\pi}\sum_{mn}\langle m|\rho|n\rangle \ \langle\alpha|\, m\rangle\langle n\,|\alpha\rangle \\ &= \frac{1}{\pi}\sum_{mn}\langle m|\rho|n\rangle \ \exp(-|\alpha|^2)\ \frac{\alpha^n\alpha^{*m}}{\sqrt{n!m!}}\ , \end{aligned} \tag{2.22}$$

α here is a complex number and could be written as $\alpha = re^{i\phi}$. Similar to the case of a Wigner function we integrate out r to find $P_q(\phi)$:

$$\begin{aligned} P_q(\phi) &= \frac{1}{\pi}\sum_{mn}\langle m|\rho|n\rangle \ \int_0^\infty dr\ r\ \exp(-r^2)\ \frac{r^{n+m}}{\sqrt{n!m!}}\ \exp\{i(n-m)\phi\} \\ &= \frac{1}{2\pi}\sum_{mn}\langle m|\rho|n\rangle \ R_q(m,n)\ \exp\{i(n-m)\phi\} \\ &= \frac{1}{2\pi} + \frac{1}{2\pi}\sum_{m\neq n}\langle m|\rho|n\rangle \ R_q(m,n)\ \exp\{i(n-m)\phi\}\ , \end{aligned} \tag{2.23}$$

where $R_q(m,n)$ is the integral of the radial part of the Q-function, given by

$$R_q(m,n) = \int_0^\infty dr\ 2r\ \exp(-r^2)\ \frac{r^{n+m}}{\sqrt{n!m!}}\ , \tag{2.24}$$

with properties: $R(m,m) = 1$ and $R(m,n) = R(n,m)$. We define a new term C_k^q as follows

$$C_k^q = \sum_{m-n=k}\langle m|\,\rho\,|n\rangle\, R_q(m,n), \tag{2.25}$$

it could be decomposed into its angular and radial part as $C_k^q = A_k^q \exp(i\Theta_q^k)$. Eq 2.23 could be further simplified to reduce it to a form similar to Eq 2.20, i.e. a superposition of different harmonic modes. The simplified form of $P_q(\phi)$ is given by

$$P_q(\phi) = \frac{1}{2\pi} + \frac{1}{\pi}\sum_{k=1}^{\infty} A_k^q \cos(k\phi - \Theta_k^q)\ . \tag{2.26}$$

This form of phase distribution derived from the Q-function is very similar to the one derived from the Wigner function, the only difference is in the radial integral part, both of these produce qualitatively similar plots.

Till now we derived $P(\phi)$ from phase space distributions, instead, we could also use

states of the harmonic oscillator which have a defined phase ϕ. Much work has been done on defining a phase operator and phase eigenstates for a harmonic oscillator [15, 16]. Many formalisms have been developed to study the phase properties of a QHO, one of the most established ones is the Susskind-Glogower (SG) formalism [17, 18]. Under this approach, we define a quantum analog $\hat{E}$ for the exponential of the phase $e^{i\phi}$. $\hat{E}$ is defined as

$$\hat{E} \equiv (\hat{n}+1)^{-\frac{1}{2}}\hat{a} \ , \tag{2.27}$$

with the eigenstates given by

$$|\phi\rangle = \sum_{n=0}^{\infty} e^{in\phi} |n\rangle \, . \tag{2.28}$$

These eigenstates $|\phi\rangle$ have a properly defined phase of ϕ. $\{|\phi\rangle\}$ form an overcomplete basis for the Hilbert space of QHO, with the resolution to unity given by

$$\frac{1}{2\pi}\int_0^{2\pi} d\phi \ |\phi\rangle \langle\phi| = 1 \ . \tag{2.29}$$

Using the phase states $|\phi\rangle$, the phase distribution for a density matrix ρ is given by [19]

$$P_p(\phi) = \frac{1}{2\pi} \langle\phi| \rho |\phi\rangle \, , \tag{2.30}$$

expanding the density matrix in the Fock basis we could further simplify the equation as follows

$$\begin{aligned} P_p(\phi) &= \frac{1}{2\pi} \langle\phi| \rho |\phi\rangle \\ &= \frac{1}{2\pi} \sum_{mn} \langle m|\rho|n\rangle \langle\phi| m\rangle\langle n |\phi\rangle \\ &= \frac{1}{2\pi} \sum_{mn} \langle m|\rho|n\rangle \ \exp\{i(n-m)\phi\} \\ &= \frac{1}{2\pi} + \frac{1}{2\pi} \sum_{m\neq n} \langle m|\rho|n\rangle \ \exp\{i(n-m)\phi\} \ . \end{aligned} \tag{2.31}$$

The form of phase distribution in Eq 2.31, similar to the previous cases, tells us that for a non-uniform phase distribution, we need coherences in the state. We define a new term C_k^p as follows

$$C_k^p = \sum_{m-n=k} \langle m| \rho |n\rangle \, , \tag{2.32}$$

for this case C_k^p is simply the sum of all elements of the subset S_k, it could be decomposed into its angular and radial part as $C_k^p = A_k^p \exp(i\Theta_p^k)$. $P_p(\phi)$ can be simplified to the following form

$$P_p(\phi) = \frac{1}{2\pi} + \frac{1}{\pi}\sum_{k=1}^{\infty} A_k^p \cos(k\phi - \Theta_k^p) \ . \tag{2.33}$$

The phase distributions in Eq 2.20 and 2.26, derived from phase space distributions were dependent on the density matrix elements along with the radial integrals $R(m,n)$. But the phase distribution derived from phase states $|\phi\rangle$ is only dependent on the density matrix elements, this helps us to understand the relation of density matrix elements to the phase distribution of the state.

We could define a new distribution $S(\phi)$ [20, 21] derived from the phase distribution $P(\phi)$, given as follows

$$S(\phi) = P(\phi) - \frac{1}{2\pi} \ . \tag{2.34}$$

This definition is more efficient as for a uniform phase distribution it takes a constant value of zero, any non-zero value indicates phase selectivity up to a certain degree. We can also use $\max\{S(\phi)\}$ as a measure of synchronization as it quantifies how peaked the phase distribution is for single and collection of oscillators [22].

The analysis done in this section regarding the phase distribution and its dependence on different types of coherences is quite general. It is applicable to any harmonic oscillator state, not just a QVdP. Now after we have established a setup for SSO and a method to measure phase-locking, all we need is to apply an external drive to the QVdP and study its phase-locking properties.

2.4 QVdP with an External Drive

The most fundamental form of synchronization is the synchronization of an oscillator to an external drive. Here the drive benefits from the free phase property of an SSO which helps it to freely modify the phase to lock it with its own phase. We apply a harmonic drive to a QVdP of the following form

$$H_d = \epsilon(e^{i\omega t}a + e^{-i\omega t}a^\dagger) \ , \tag{2.35}$$

where ϵ is the strength of the drive and ω is its frequency. The master equation for the driven QVdP is given by

$$\dot{\tilde{\rho}} = -i\left[\omega_0 a^\dagger a + \epsilon(e^{i\omega t}a + e^{-i\omega t}a^\dagger), \tilde{\rho}\right] + \gamma_g \mathcal{D}[a^\dagger]\tilde{\rho} + \gamma_l \mathcal{D}[a^2]\tilde{\rho}. \tag{2.36}$$

Given that we are studying the phase locking of the oscillator to a drive, it would be

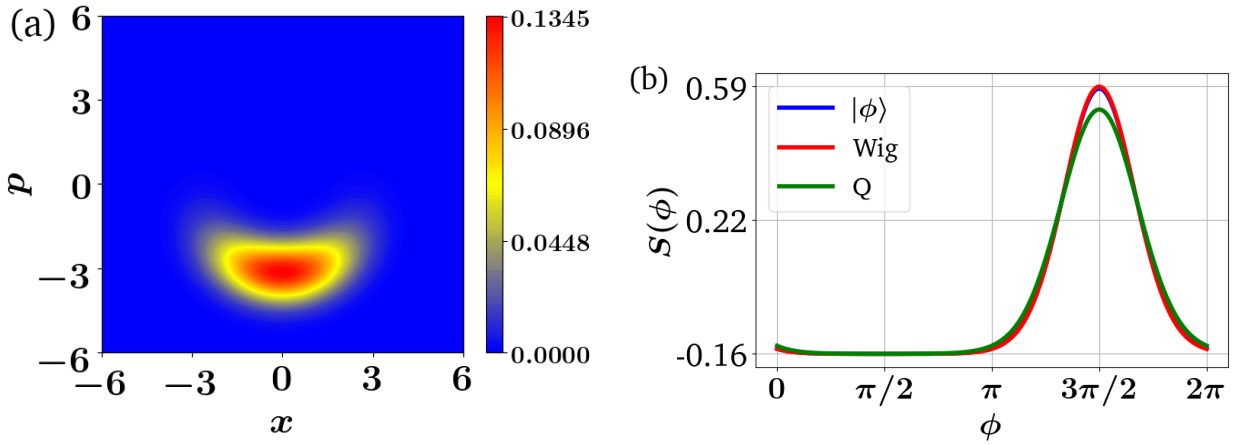

Figure 2.4: When we apply an external drive to a QVdP this leads to the locking of its phase to that of the drive. For the master equation of a driven QVdP in Eq 2.38 with $\gamma_g/\gamma_l = 5$ and $\Delta = 0$, we get a steady state ρ_{ss}. (a) The Wigner function for ρ_{ss} becomes concentrated around the phase $3\pi/2$ unlike the one in fig 2.3 for undriven QVdP which is circularly symmetric. (b) The phase distributions $P(\phi)$ derived from the Wigner function (Red), Q-function (Green), and phase states $|\phi\rangle$ (Blue), are all peaked at $3\pi/2$. This shows that relative to the phase of the drive, the oscillator's phase is locked.

beneficial to transform to a frame rotating with the drive. The state in this frame is given by following unitary transform

$$\rho = \exp\left(i\omega_0 a^\dagger a\right)\tilde{\rho}\exp\left(-i\omega_0 a^\dagger a\right), \tag{2.37}$$

master equation for the QVdP in the rotating frame is given by [9]

$$\dot{\rho} = -i\left[-\Delta\hat{a}^\dagger\hat{a} + \epsilon(\hat{a} + \hat{a}^\dagger), \rho\right] + \gamma_1 \mathcal{D}[\hat{a}^\dagger]\rho + \gamma_2 \mathcal{D}[\hat{a}^2]\rho \tag{2.38}$$

where Δ is the detuning between the drive's frequency and the natural frequency of the oscillator. When the strength of the drive is zero, the master equation gives us a steady state similar to Eq 2.4 with the circularly symmetric Wigner function, similar to the fig 2.3. The application of the drive leads to synchronization of the QVdP [9, 10] and it develops a

phase relation with the drive. This could be seen from fig 2.4, where we see a non-uniform distribution of phase for the driven QVdP.

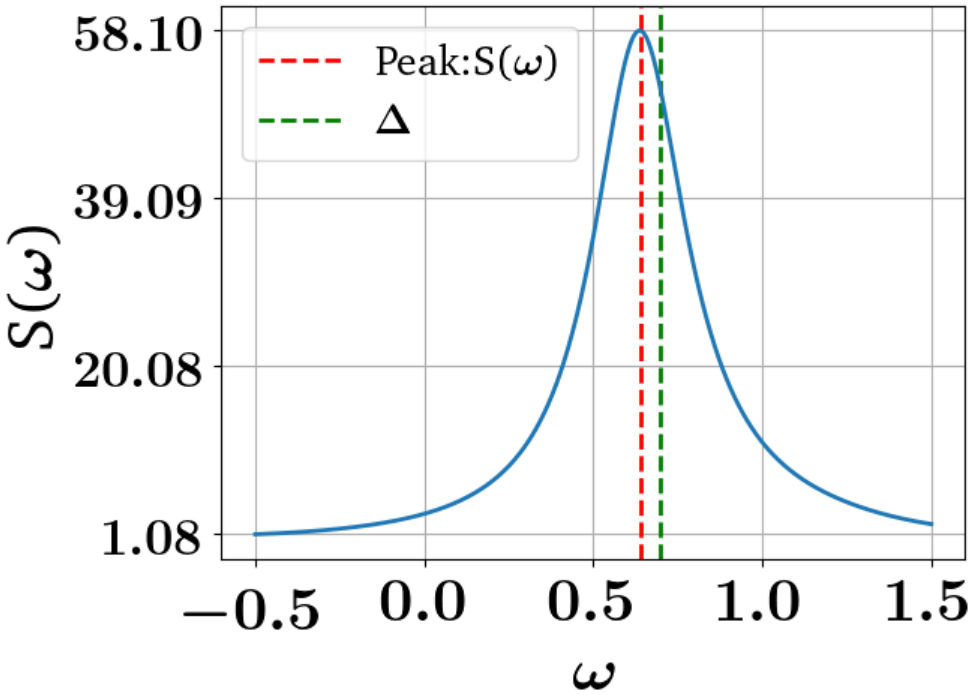

Figure 2.5: Power spectrum for the steady state of a driven QVdP in the reference frame of the drive's frequency, with $\gamma_l/\gamma_g = 0.1, \Delta = 0.7$ and $\epsilon = 1$. As the power spectrum is calculated for the QVdP master equation 2.38 which is in the drive's frame, naturally the peak is located at detuning value Δ. But due to frequency entrainment of the drive, the peak appears closer to zero, this is a signature of synchronization behavior.

Apart from studying the phase space of the oscillator, we could also analyze its power spectrum to look for signatures of synchronization. Given an oscillator with natural frequency ω_0 is being driven with a frequency ω, for synchronization to exist we expect the power spectrum of the oscillator to shift towards the drive's frequency. The power spectrum for the QVdP in the drive's frame when $\epsilon = 0$ shows a peak at the detuning value Δ, as there is no frequency entrainment. When we increase the value of ϵ, we expect the frequency of the QVdP to come closer to that of the drive. As the master equation 2.38 is in the drive's frame, this means that the peak of the power spectrum would shift closer to zero. The power spectrum for the oscillator is given by

$$S(\omega) = \int_{-\infty}^{\infty} dt\, e^{i\omega t} \left\langle a^\dagger(t) a(0) \right\rangle \ , \tag{2.39}$$

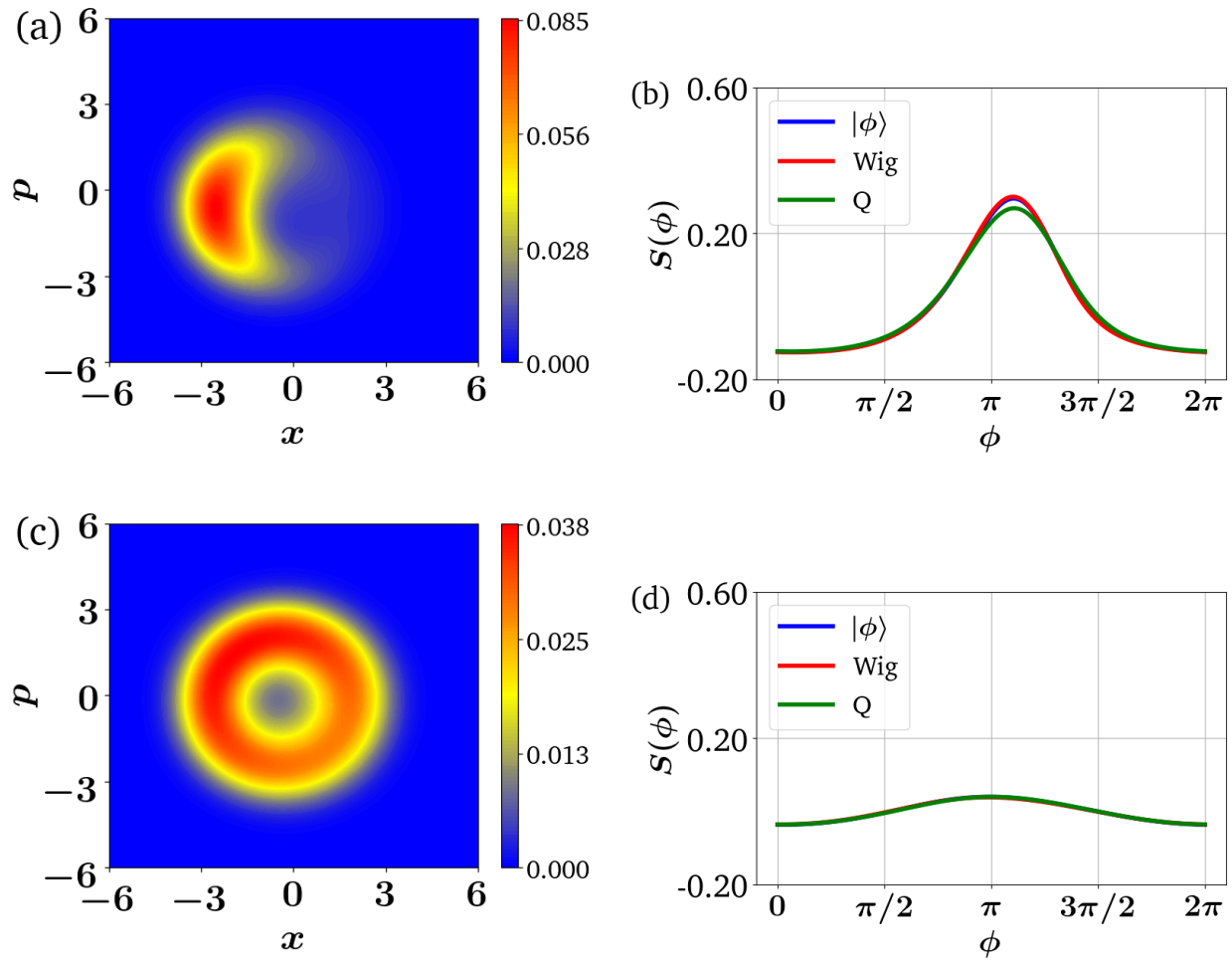

Figure 2.6: As we increase the detuning between the QVdP and drive, the synchronization becomes weaker and the phase distribution starts to be more uniformly distributed. A driven QVdP with $\gamma_l/\gamma_g = 0.1$, $\epsilon = 1$, (a,b) $\Delta = 0.7$ and (c,d) $\Delta = 3$. For $\Delta = 0.7$ the phase-locking survives with an increase in the spread of the Wigner function compared to fig 2.4, whereas for $\Delta = 3$ the Wigner function becomes nearly circularly symmetric similar to fig 2.3.

where $\langle a^\dagger(t)a(0)\rangle$ is the first order correlation function, calculated from the Quantum Regression Theorem [11, 23]. As we can see from fig 2.39, the peak of the power spectrum for a driven QVdP doesn't align with the detuning. The drive tries to decrease the detuning in the new observed frequency of QVdP.

As we keep increasing the detuning between the QVdP and drive, the degree of phase locking decreases as they are not able to maintain a constant phase relationship for large differences in frequency [9]. From fig 2.4 and 2.6, we could see that as the value of Δ increases the Wigner function starts to spread out and the phase distribution becomes less peaked.

Chapter 3

Synchronization between Two Harmonic Oscillators

In the last chapter, we studied how we could synchronize an oscillator to an external drive. This kind of synchronization could be seen as unidirectional coupling where only the oscillator's phase is being influenced and the drive is unaffected. Instead of this, we could also study the synchronization between two coupled oscillators in which both systems involved affect each other [24]. For this case, phase-locking means that the two units develop a relation such that the relative phase, defined as $\phi = (\phi_1 - \phi_2)$, shows phase selectivity.

A system of two uncoupled QVdP has the following master equation [24]

$$\dot{\rho} = -i\left[H_0, \rho\right] + \sum_{i=1,2} \gamma_g^{(i)} \mathcal{D}\left[a_i^\dagger\right] \rho + \gamma_l^{(i)} \mathcal{D}\left[a_i^2\right] \rho, \tag{3.1}$$

where $H_0 = \sum_{i=1,2} \omega_i a_i^\dagger a_i$. The joint density matrix for the uncoupled system has the form $\rho = \rho_1 \otimes \rho_2$. As the steady-state density matrix for a QVdP is diagonal in the Fock basis, the joint steady-state density matrix ρ_{ss} will be diagonal in the joint Fock basis for the system. We would need to supply a relevant coupling to the system for synchronizing the oscillators. For this, we would also need to come up with a method to examine the relative phase between two oscillators.

The chapter is organized as follows, in sec 3.1 we derive the equation for relative phase

distribution between two quantum harmonic oscillators from their joint phase space distribution. In sec 3.2 we study the synchronization of two QVdP due to a coherent interaction. Finally in sec 3.3 we look at the synchronization due to dissipative coupling between a pair of QVdP.

3.1 Relative Phase Distribution of Two QHO

In sec 2.3 we saw how we could plot the phase distribution of a QHO from its quasiprobability phase space distribution and also from its phase states $|\phi\rangle$. Now we have to study the synchronization properties of two oscillators, instead of analyzing separate phase spaces for both oscillators, we look at the joint phase space because it captures all correlations that could exist between the two systems.

The two-mode Wigner function for a joint state ρ of two quantum harmonic oscillators is defined as [25]

$$W(x_1, p_1, x_2, p_2) = \frac{1}{\pi^2} \int_{-\infty}^{\infty} dy_1 \; dy_2 \; e^{2i(p_1 y_1 + p_2 y_2)} \times \langle x_1 - y_1, x_2 - y_2 | \rho | x_1 + y_1, x_2 + y_2 \rangle. \quad (3.2)$$

Expanding ρ in the joint Fock basis and using the Wigner function W_{mn} for $|m\rangle \langle n|$ as given in Eq 2.16, we could write the two-mode Wigner function as

$$W(x_1, p_1, x_2, p_2) = \sum_{m_1 n_1 m_2 n_2} \langle m_1 m_2 | \rho | n_1 n_2 \rangle W_{m_1 n_1}(x_1, p_1) W_{m_2 n_2}(x_2, p_2). \quad (3.3)$$

For the study of synchronization between the oscillators we are interested in the distribution for the relative phase, i.e. $\phi = (\phi_1 - \phi_2)$. To extract the information about relative phase ϕ we do the following coordinate transforms of the Wigner function:

$$(x_1, p_1, x_2, y_2) \to (r_1, \phi_1, r_2, \phi_2) \to (r_1, r_2, \phi, \kappa)$$

The first transformation is from cartesian to polar coordinates, the second transformation gives us a distribution in phase sum and difference, with $\kappa = (\phi_1 + \phi_2)$. Now we have a joint probability distribution in four variables, we integrate out r_1, r_2 and κ, with appropriate Jacobians, to get the marginal probability distribution $P(\phi)$. The relative phase distribution is given by

$$
\begin{aligned}
P_w(\phi) &= \sum_{m_1 n_1 m_2 n_2} \langle m_1 m_2|\rho|n_1 n_2\rangle \int_0^\infty dr_1\ r_1 \int_0^\infty dr_2\ r_2 \int_0^{4\pi} d\kappa\ \frac{1}{2} W_{m_1 n_1}(r_1,\phi_1) W_{m_2 n_2}(r_2,\phi_2) \\
&= \sum_{m_1 n_1 m_2 n_2} \langle m_2 m_2|\rho|n_1 n_1\rangle \frac{1}{(2\pi)^2} R_w(m_1,n_1) R_w(m_2,n_2) \times \\
&\quad \int_0^{4\pi} d\kappa\ \frac{1}{2}\ \exp\left(i[(n_1+n_2)-(m_1+m_2)]\frac{\kappa}{2}\right) \exp\left(i[(n_1-n_2)-(m_1-m_2)]\frac{\phi}{2}\right).
\end{aligned}
\tag{3.4}
$$

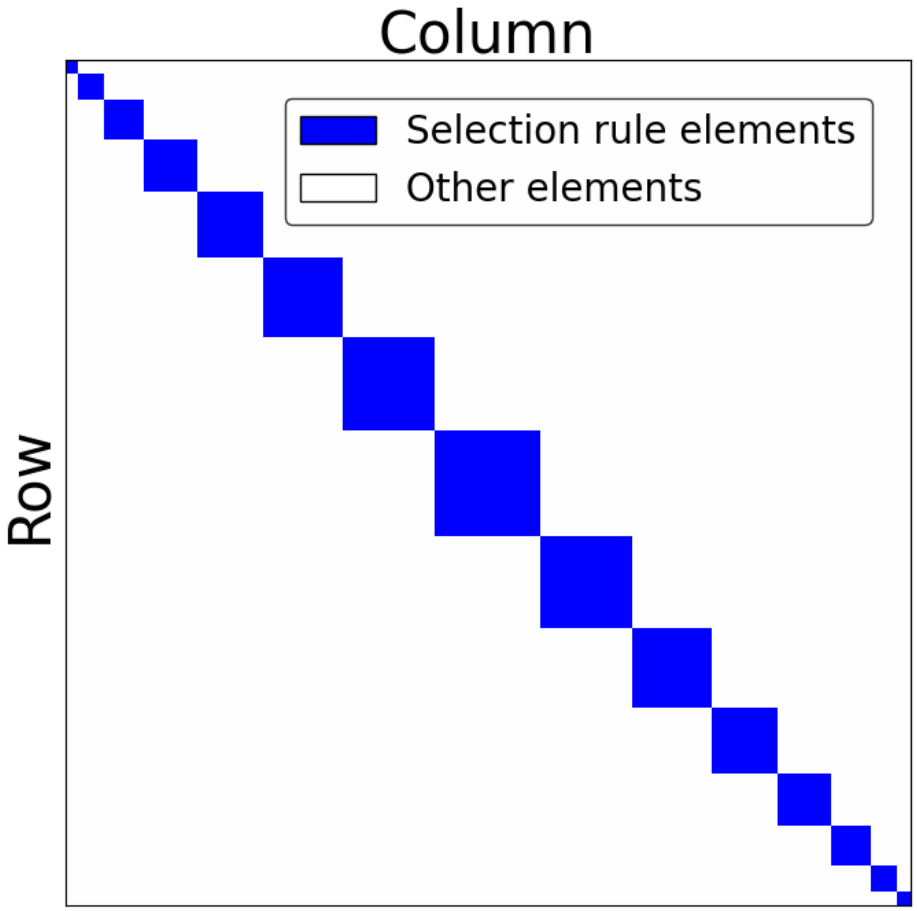

Figure 3.1: The relative phase distribution between two oscillators is determined by only those density matrix elements $\langle m_1, m_2|\,\rho\,|n_1, n_2\rangle$ that satisfy $(m_1+m_2)=(n_1+n_2)$. For the density matrix in joint Fock basis with ordering such that states with the same total occupation are grouped together, these selection rule elements form a block diagonal structure as shown in the figure.

The integral with respect to κ survives only for those density matrix elements $\langle m_1, m_2| \rho |n_1, n_2\rangle$ terms which satisfy the condition:

$$m_1 + m_2 = n_1 + n_2, \tag{3.5}$$

here we obtain a selection rule over the joint density matrix elements which determines the relative phase distribution between two QHO, unlike the case of a single QHO where all density matrix elements contributed to $P(\phi)$, as in Eq 2.17, 2.31 and 2.23. In a density matrix written in joint Fock basis such that the basis elements are reordered to group the states with same total occupation together $\{|0,0\rangle ; |0,1\rangle , |1,0\rangle ; |0,2\rangle , |1,1\rangle , |2,0\rangle ; ...\}$, the matrix elements that follow the selection rule form a block diagonal structure, as could be seen in fig 3.1. The joint Hilbert space could be divided into subspaces with a fixed total occupation, the selection rule elements exist as coherences and populations within these subspaces, that is why we observe a block diagonal structure.

The simplified form of the distribution is given by:

$$P_w(\phi) = \frac{1}{2\pi} + \frac{1}{2\pi} \sum_{\substack{m_1+m_2=n_1+n_2 \\ m_1 \neq n_1}} \langle m_1 m_2|\rho|n_1 n_2\rangle \; I_w(m_1, m_2, n_1, n_2) \; \exp\{i(n_1 - m_1)\phi\} \tag{3.6}$$

where: $I_w(m_1, m_2, n_1, n_2) = R_w(m_1, n_1)R_w(m_2, n_2)$. As we can see from the above equation the relative phase distribution for a state diagonal in the joint Fock basis is uniform, indicating no phase locking, that is why the steady state of Eq 3.1 also possesses no phase locking. For phase selectivity to exist we need off-diagonal coherence terms that satisfy the selection rule in Eq 3.5. In other words, phase locking between two QHO requires coherence between joint Fock states with the same total occupation. We define a new term C_k^w as follows

$$C_k^w = \sum_{m_1 - n_1 = k} \langle m_1, m_2| \rho |n_1, n_2\rangle \, I_w(m_1, m_2, n_1, n_2), \tag{3.7}$$

it could be decomposed into its angular and radial part as $C_k^w = A_k^w \exp(i\Theta_w^k)$. Simplifying Eq 3.6 further we get

$$P_w(\phi) = \frac{1}{2\pi} + \frac{1}{2\pi} \sum_{\substack{m_1+m_2=n_1+n_2 \\ m_1 \neq n_1}} \langle m_1 m_2|\rho|n_1 n_2\rangle \; I_w(m_1, m_2, n_1, n_2) \; \exp\{i(n_1 - m_1)\phi\}$$

$$
\begin{aligned}
&= \frac{1}{2\pi} + \frac{1}{2\pi} \sum_{\substack{m_1+m_2=n_1+n_2 \\ m_1>n_1}} \langle m_1 m_2|\rho|n_1 n_2\rangle \; I_w(m_1, m_2, n_1, n_2) \; \exp\{i(n_1 - m_1)\phi\} + h.c. \\
&= \frac{1}{2\pi} + \frac{1}{2\pi} \sum_{k=1}^{\infty} \left[\exp(-ik\phi) \sum_{m_1 - n_1 = k} \langle m_1, m_2| \, \rho \, |n_1, n_2\rangle \, I_w(m_1, m_2, n_1, n_2) \right] + h.c. \\
&= \frac{1}{2\pi} + \frac{1}{2\pi} \sum_{k=1}^{\infty} [C_k^w \exp(-ik\phi)] + h.c. \\
&= \frac{1}{2\pi} + \frac{1}{2\pi} \sum_{k=1}^{\infty} [A_k^w \exp\{-i(k\phi - \Theta_k^w)\}] + h.c. \\
&= \frac{1}{2\pi} + \frac{1}{\pi} \sum_{k=1}^{\infty} A_k^w \cos(k\phi - \Theta_k^w) \; . \qquad (3.8)
\end{aligned}
$$

We are able to write the relative phase distribution as a superposition of different harmonic modes. The selection rule elements determining the relative phase distribution form a set S, this set could be further divided into subsets S_k based on classification $\langle m_1 + k, m_2| \, \rho \, |m_1, m_2 + k\rangle$. Elements of the subset S_k contribute to the k-th harmonic of the relative phase distribution. The joint density matrix for the two oscillators when written in the joint Fock basis with lexicographic order, i.e. $\{|0,0\rangle, |0,1\rangle, |0,2\rangle, ...; |1,0\rangle, |1,1\rangle, ...; ...\}$, the subsets $\{S_k\}$ form separate bands of elements as could be seen in fig 3.2.

Apart from using the Wigner function, we could also use the two-mode Q-function to plot the relative phase distribution. For a given state ρ of two quantum harmonic oscillators, the two-mode Q-function is defined as

$$
Q(\alpha_1, \alpha_2) = \frac{1}{\pi^2} \langle \alpha_1, \alpha_2| \, \rho \, |\alpha_1, \alpha_2\rangle \qquad (3.9)
$$

where $|\alpha\rangle$ is the QHO coherent state defined as:$|\alpha\rangle = e^{-\frac{|\alpha|^2}{2}} \sum_{n=0}^{\infty} \frac{\alpha^n}{\sqrt{n!}} |n\rangle$. Expanding Eq 3.9 in the joint Fock basis we get:

$$
\begin{aligned}
Q &= \frac{1}{\pi^2} \sum_{m_1 n_1 m_2 n_2} \langle m_1 m_2|\rho|n_1 n_2\rangle \; \langle \alpha_1 |m_1\rangle \langle \alpha_2 |m_2\rangle \langle n_1 |\alpha_1\rangle \langle n_2 |\alpha_2\rangle \\
&= \frac{1}{\pi^2} \sum_{m_1 n_1 m_2 n_2} \langle m_1 m_2|\rho|n_1 n_2\rangle \; \exp(-|\alpha_1|^2) \; \frac{\alpha_1^{n_1} \alpha_1^{*m_1}}{\sqrt{n_1! m_1!}} \; \exp(-|\alpha_2|^2) \; \frac{\alpha_2^{n_2} \alpha_2^{*m_2}}{\sqrt{n_2! m_2!}}. \qquad (3.10)
\end{aligned}
$$

Here α_1 and α_2 are complex numbers and could be written as $\alpha_1 = r_1 e^{i\phi_1}$ and $\alpha_2 = r_2 e^{i\phi_2}$,

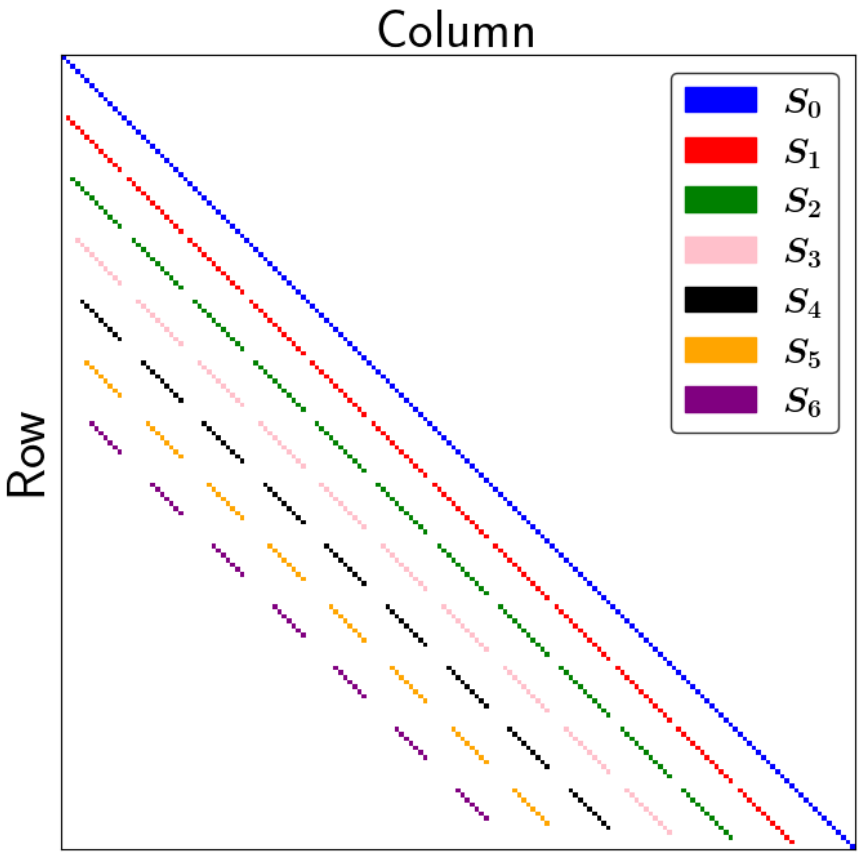

Figure 3.2: The selection rule elements could be further divided into subsets S_k with elements of the form $\langle m_1 + k, m_2 | \rho | m_1, m_2 + k \rangle$. The elements of a subset S_k contribute to the k-th harmonic mode of the relative phase distribution. For the density matrix in joint Fock basis with lexicographic ordering, these subsets form separate bands as shown in the figure.

this gives us:

$$Q = \frac{1}{\pi^2} \sum_{m_1 n_1 m_2 n_2} \langle m_1 m_2 | \rho | n_1 n_2 \rangle \exp(-r_1^2) \frac{r_1^{n_1+m_1}}{\sqrt{n_1! m_1!}} \exp(-r_2^2) \frac{r_2^{n_2+m_2}}{\sqrt{n_2! m_2!}} \exp\{i(n_1 - m_1)\phi_1\} \exp\{i(n_2 - m_2)\phi_2\}. \tag{3.11}$$

Now transforming the equation in terms of angle difference and angle sum we get:

$$Q = \frac{1}{\pi^2} \sum_{m_1 n_1 m_2 n_2} \langle m_1 m_2 | \rho | n_1 n_2 \rangle \ \exp(-r_1^2) \ \frac{r_1^{n_1+m_1}}{\sqrt{n_1! m_1!}} \ \exp(-r_2^2) \ \frac{r_2^{n_2+m_2}}{\sqrt{n_2! m_2!}}$$
$$\exp\left(i\{(n_1 + n_2) - (m_1 + m_2)\}\frac{\kappa}{2}\right) \exp\left(i\{(n_1 - n_2) - (m_1 - m_2)\}\frac{\phi}{2}\right) \tag{3.12}$$

To obtain $P(\phi)$ we integrate out r_1, r_2 and κ as follows

$$P(\phi) = \frac{1}{\pi^2} \sum_{m_1 n_1 m_2 n_2} \langle m_1 m_2|\rho|n_1 n_2\rangle \int_0^\infty dr_1 \; r_1 \exp(-r_1^2) \; \frac{r_1^{n_1+m_1}}{\sqrt{n_1! m_1!}} \; \int_0^\infty dr_2 \; r_2 \exp(-r_2^2) \; \frac{r_2^{n_2+m_2}}{\sqrt{n_2! m_2!}}$$
$$\int_0^{4\pi} d\kappa \; \frac{1}{2} \exp\left(i\{(n_1+n_2)-(m_1+m_2)\}\frac{\kappa}{2}\right) \exp\left(i\{(n_1-n_2)-(m_1-m_2)\}\frac{\phi}{2}\right). \tag{3.13}$$

Integration over κ gives us the same selection rule as in Eq 3.5, over the density matrix elements. This simplifies the equation to be

$$P(\phi) = \frac{1}{2\pi} + \frac{1}{2\pi} \sum_{\substack{m_1+m_2=n_1+n_2 \\ m_1 \neq n_1}} \langle m_1 m_2|\rho|n_1 n_2\rangle \; I_q(m_1, m_2, n_1, n_2) \; \exp[i((n_1-m_1)\phi)] \tag{3.14}$$

where $I_q(m_1, m_2, n_1, n_2) = R_q(m_1, n_1) R_q(m_2, n_2)$ and $R_q(m, n)$ is the same as defined in Eq 2.24. We define a new term C_k^q as follows

$$C_k^q = \sum_{m_1 - n_1 = k} \langle m_1, m_2| \, \rho \, |n_1, n_2\rangle \; I_q(m_1, m_2, n_1, n_2), \tag{3.15}$$

it could be decomposed into its angular and radial part as $C_k^q = A_k^q \exp(i\Theta_q^k)$. Simplifying Eq 3.14 further we get

$$P_q(\phi) = \frac{1}{2\pi} + \frac{1}{\pi} \sum_{k=1}^{\infty} A_k^q \cos(k\phi - \Theta_k^q) \tag{3.16}$$

We could also use the QHO phase states $|\phi\rangle$ as defined in Eq 2.28 to find the relative phase distribution between two harmonic oscillators. The joint probability distribution for the individual phases of both the oscillators is given by [26]

$$\begin{aligned} P(\phi_1, \phi_2) &= \frac{1}{(2\pi)^2} \langle \phi_1, \phi_2| \, \rho \, |\phi_1, \phi_2\rangle \\ &= \frac{1}{(2\pi)^2} \sum_{m_1 n_1 m_2 n_2} \langle m_1 m_2|\rho|n_1 n_2\rangle \; \langle \phi_1 \, |m_1\rangle \, \langle \phi_2 \, |m_2\rangle \, \langle n_1 \, |\phi_1\rangle \, \langle n_2 \, |\phi_2\rangle \\ &= \frac{1}{(2\pi)^2} \sum_{m_1 n_1 m_2 n_2} \langle m_1 m_2|\rho|n_1 n_2\rangle \exp\{i(n_1-m_1)\phi_1\} \exp\{i(n_2-m_2)\phi_2\}. \end{aligned} \tag{3.17}$$

To find the relative phase distribution we do a variable transform from (ϕ_1, ϕ_2) to (ϕ, κ) and

integrate out κ:

$$P_p(\phi) = \frac{1}{(2\pi)^2} \sum_{m_1 n_1 m_2 n_2} \langle m_1 m_2|\rho|n_1 n_2\rangle \int_0^{4\pi} d\kappa \, \frac{1}{2} \exp\left(i[(n_1+n_2)-(m_1+m_2)]\frac{\kappa}{2}\right) \exp\left(i[(n_1-n_2)-(m_1-m_2)]\frac{\phi}{2}\right)$$

Here also we get the same selection rule over density matrix elements as in Eq 3.5 because of integration over κ. We define a new term C_k^p as follows

$$C_k^p = \sum_{m_1-n_1=k} \langle m_1, m_2|\, \rho \,|n_1, n_2\rangle \,, \tag{3.18}$$

it could be decomposed into its angular and radial part as $C_k^p = A_k^p \exp(i\Theta_p^k)$. The simplified form for $P_p(\phi)$ similar to Eq 3.8 and 3.16 could be written as

$$P_p(\phi) = \frac{1}{2\pi} + \frac{1}{\pi} \sum_{k=1}^{\infty} A_k^p \cos(k\phi - \Theta_k^p). \tag{3.19}$$

The relative phase distributions derived from phase space representations like Wigner and Q function were dependent on density matrix elements and also radial integrals $I(m_1, m_2, n_1, n_2)$. The distribution Eq 3.19 derived from phase states $\{|\phi\rangle\}$ has dependence only on density matrix elements, this could help us better understand how the nature of relative phase is affected by the state of the system.

3.2 Coherent Coupling

To synchronize the two QVdP we need to introduce a coupling between them such that it generates coherences as per the selection rule of Eq 3.5, in the steady state density matrix. One of the standard forms of coupling between two oscillators is a coherent exchange interaction of the form

$$H_c = \gamma_c(a_1^\dagger a_2 + a_1 a_2^\dagger), \tag{3.20}$$

where γ_c is the coupling strength. Introducing this form of coupling between two QVdP, we obtain a new master equation of the form

$$\dot{\rho} = -i\left[\sum_{i=1,2}\omega_i a_i^\dagger a_i + \gamma_c(a_1^\dagger a_2 + a_1 a_2^\dagger), \rho\right] + \sum_{i=1,2}\gamma_g^{(i)}\mathcal{D}\left[a_i^\dagger\right]\rho + \gamma_l^{(i)}\mathcal{D}\left[a_i^2\right]\rho. \tag{3.21}$$

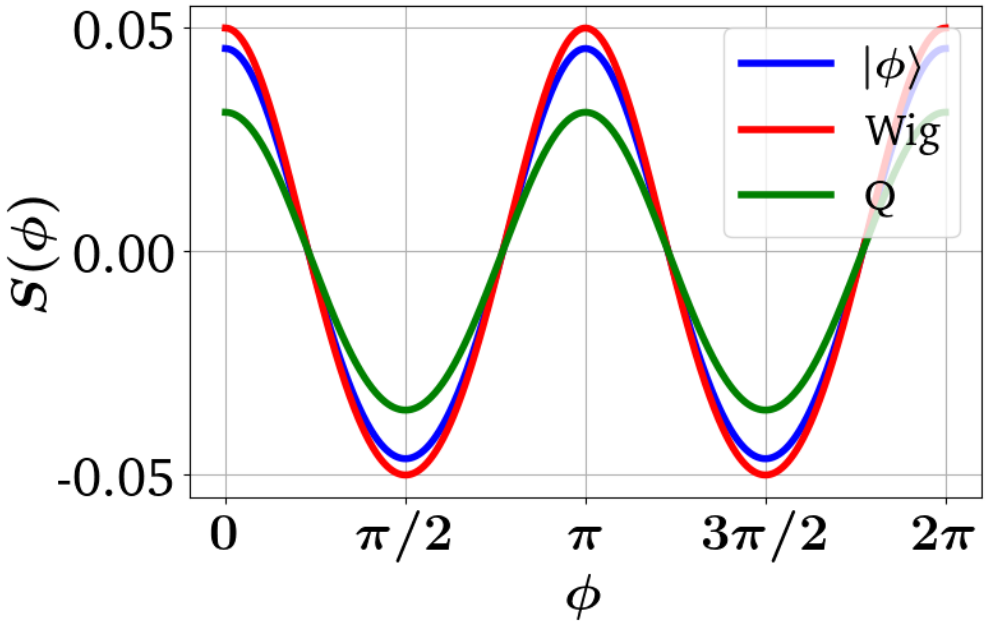

Figure 3.3: Coherent coupling of the form $(a_1^\dagger a_2 + a_1 a_2^\dagger)$ produces a non-uniform relative phase distribution between the oscillators with two peaks at 0 and π. Here we have chosen the parameters $\gamma_g = 1, \gamma_l = 0.2, \gamma_c = 1$ and $\omega_1 = \omega_2 = 1$. This interaction generates coherences as per the selection rule 3.5 leading to phase locking between the QVdP.

The master equation 3.21 produces a steady state ρ_{ss} which has a non-uniform relative phase distribution [10], as could be seen in fig 3.3. This means that for a system of two QVdP, coherent coupling of the form $(a_1^\dagger a_2 + a_1 a_2^\dagger)$ produces the selection rule elements that lead to phase-locking, as could be seen in fig 3.4. The distribution produced by all three methods is nearly similar with aligned peaks. All distributions are bimodal, this hints to us that the elements of the subset S_2 are dominant in ρ_{ss}, i.e. A_k is largest for k=2. This could be seen from fig 3.4, where we see that major contributions for the distribution come from S_2 and S_4, amongst which S_2 is dominant.

Coherent coupling leads to phase locking between the oscillators giving $\phi = (\phi_1 - \phi_2)$ a non-uniform distribution in the steady state ρ_{ss}. But if we look at the phase distribution

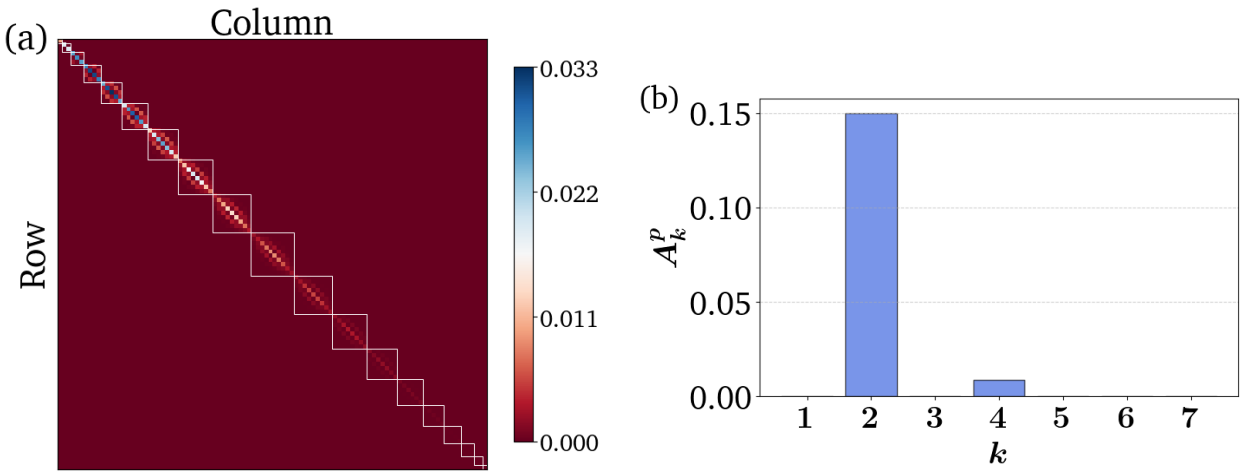

Figure 3.4: The steady state ρ_{ss} for two coherently coupled QVdP has coherences within the conserved total occupation subspaces, i.e. the coherences following the selection rule. This could be seen from (a) which is the color plot for the absolute value of density matrix elements in reordered joint Fock basis, similar to fig 3.1. As the relative phase distribution produced by ρ_{ss} is bimodal, we can see in (b) that the S_2 is the dominant subset with the largest value of A_k^p. This means that the dominant harmonic mode is $\cos(2\phi)$. Here we have chosen the parameters $\gamma_g = 1, \gamma_l = 0.2, \gamma_c = 1$ and $\omega_1 = \omega_2 = 1$.

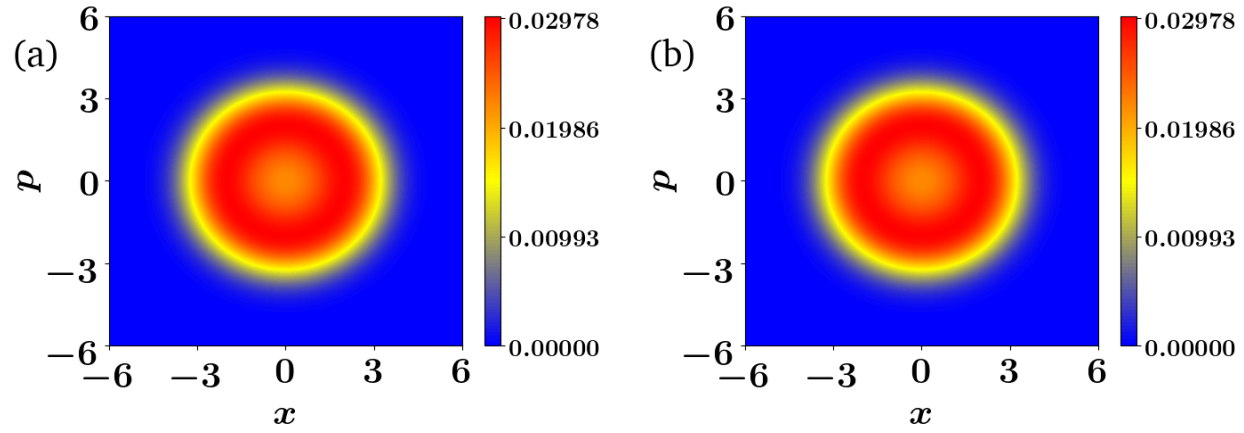

Figure 3.5: Coherent coupling produces a non-uniform distribution for the relative phase ϕ, the individual phases for each oscillator are still free with a uniform distribution. This could be seen from the Wigner distributions for $\mathrm{Tr}_2(\rho_{ss})$ (a) and $\mathrm{Tr}_1(\rho_{ss})$ (b), both are circularly symmetric about the origin signifying free phases ϕ_1 and ϕ_2. Here we have chosen the parameters $\gamma_g = 1, \gamma_l = 0.2, \gamma_c = 1$ and $\omega_1 = \omega_2 = 1$.

for individual phases ϕ_1 and ϕ_2 calculated from individual density matrices $\mathrm{Tr}_2(\rho_{ss})$ and $\mathrm{Tr}_1(\rho_{ss})$, respectively, we see that those phases are still uniformly distributed, as could be

seen in fig 3.5. This means that coherent coupling only generates global coherences not any local coherences for each oscillator. Both, $\mathrm{Tr}_2(\rho_{ss})$ and $\mathrm{Tr}_1(\rho_{ss})$ are diagonal in their Fock basis.

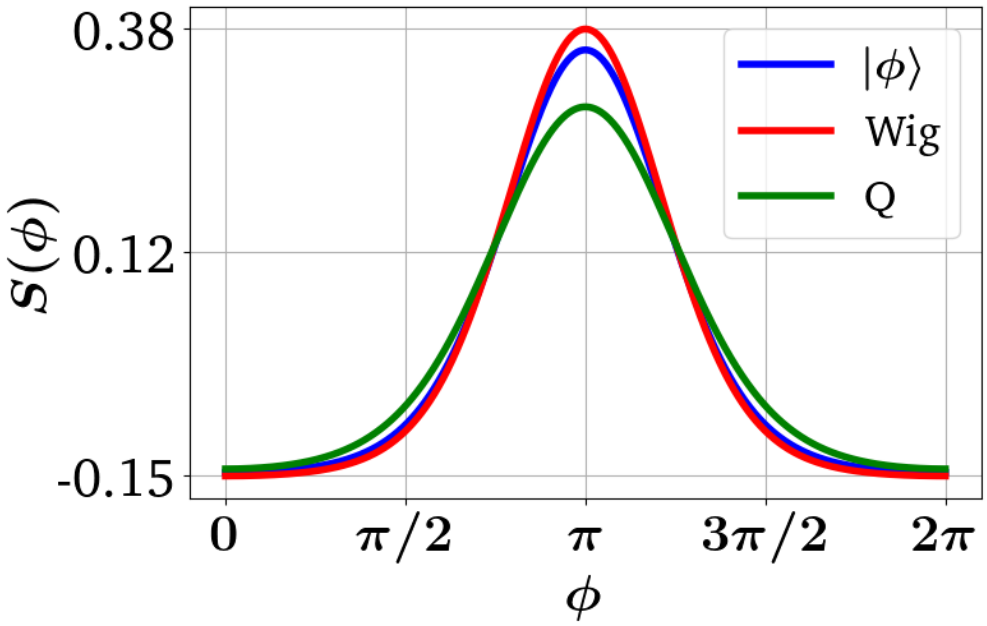

Figure 3.6: Dissipative coupling of the form $\mathcal{D}[a_1 + a_2]$ produces a non-uniform relative phase distribution between the oscillators with two peaks at π. Here we have chosen the parameters $\gamma_g = 1, \gamma_l = 0.2, \gamma_d = 1$ and $\omega_1 = \omega_2 = 1$. This interaction generates coherences as per the selection rule 3.5 leading to phase locking between the QVdP.

3.3 Dissipative Coupling

In sec 3.2 we saw how we could synchronize two oscillators with the help of a coherent coupling of the form $(a_1^\dagger a_2 + a_1 a_2^\dagger)$ introduced in the hamiltonian. Additionally, we could also use a dissipative coupling introduced due to a correlated Lindbladian dissipator. One of the standard examples of this type of coupling is a correlated one photon loss dissipator of the form $\mathcal{D}[a_1 + a_2]$ [24, 25]. The complete master equation for two QVdP coupled with this type of coupling is

$$\dot{\rho} = -i\left[\sum_{i=1,2} \omega_i a_i^\dagger a_i, \rho\right] + \left(\sum_{i=1,2} \gamma_g^{(i)} \mathcal{D}\left[a_i^\dagger\right] \rho + \gamma_l^{(i)} \mathcal{D}\left[a_i^2\right] \rho\right) + \gamma_d \mathcal{D}[a_1 + a_2], \tag{3.22}$$

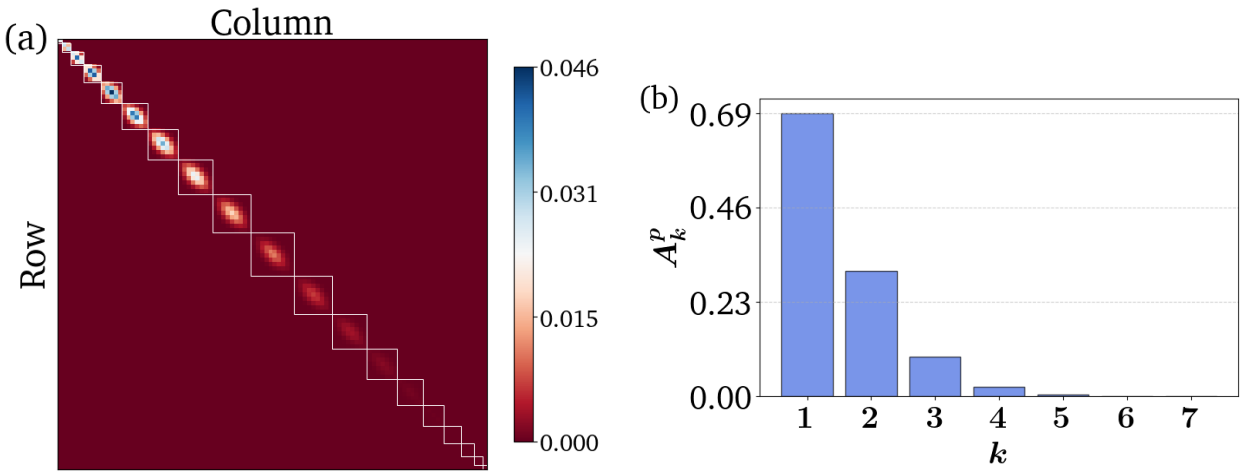

Figure 3.7: The steady state ρ_{ss} for two dissipatively coupled QVdP has coherences within the conserved total occupation subspaces, i.e. the coherences following the selection rule. This could be seen from (a) which is the color plot for the absolute value of density matrix elements in reordered joint Fock basis, similar to fig 3.1. As the relative phase distribution produced by ρ_{ss} is unimodal, we can see in (b) that the S_1 is the dominant subset with the largest value of A_k^p. This means that the dominant harmonic mode is $\cos(\phi)$. Here we have chosen the parameters $\gamma_g = 1, \gamma_l = 0.2, \gamma_d = 1$ and $\omega_1 = \omega_2 = 1$.

where γ_d is the strength of dissipative coupling. The steady-state ρ_{ss} for master equation 3.22 has a non-uniform relative phase distribution as could be seen in fig 3.6. This means that the dissipative coupling $\mathcal{D}[a_1 + a_2]$ generates coherences as per the selection rule in the steady state, as could be seen from fig 3.7.

The distribution produced by all three methods is nearly similar with aligned peaks. All distributions are unimodal, this hints to us that the elements of the subset S_1 are dominant in ρ_{ss}, i.e. A_k is largest for k=1. This could be seen from fig 3.7, where we see that contributions for the distribution come from many subsets, amongst which S_1 is dominant.

Dissipative coupling leads to phase locking between the oscillators giving $\phi = (\phi_1 - \phi_2)$ a non-uniform distribution in the steady state ρ_{ss}. But if we look at the phase distribution for individual phases ϕ_1 and ϕ_2 calculated from individual density matrices $\mathrm{Tr}_2(\rho_{ss})$ and $\mathrm{Tr}_1(\rho_{ss})$, respectively, we see that those phases are still uniformly distributed, as could be seen in fig 3.8. This means that even dissipative coupling only generates global coherences not any local coherences for each oscillator. Both, $\mathrm{Tr}_2(\rho_{ss})$ and $\mathrm{Tr}_1(\rho_{ss})$ are diagonal in their Fock basis.

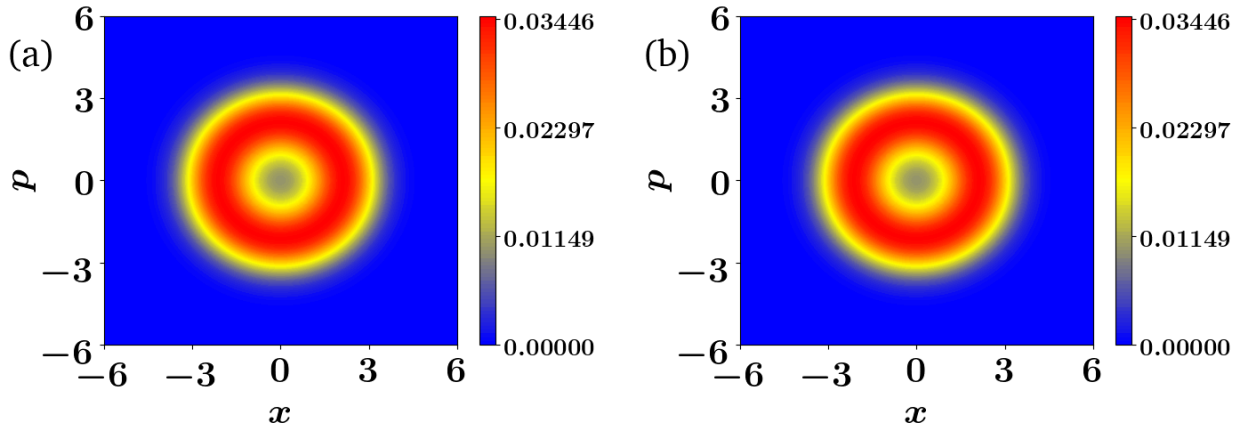

Figure 3.8: Dissipative coupling produces a non-uniform distribution for the relative phase ϕ, the individual phases for each oscillator are still free with a uniform distribution. This could be seen from the Wigner distributions for $\mathrm{Tr}_2(\rho_{ss})$ (a) and $\mathrm{Tr}_1(\rho_{ss})$ (b), both are circularly symmetric about the origin signifying free phases ϕ_1 and ϕ_2. Here we have chosen the parameters $\gamma_g = 1, \gamma_l = 0.2, \gamma_d = 1$ and $\omega_1 = \omega_2 = 1$.

Chapter 4

Synchronization of Spin to a Drive

The last two chapters were concerned with the synchronization of continuous variable systems which have a clear classical analog. In this chapter, we study the synchronization properties of purely quantum mechanical discrete-variable spin systems. According to the general prescription of synchronization studies, first, we establish a free phase limit cycle by supplying the spin system with loss and gain dissipators. Then we drive the system or couple it to a second quantum unit to study the phase-locking behavior.

The chapter is organized as follows, in sec 4.1 we model a self-sustained oscillator from a spin-1 system with an equatorial limit cycle. In sec 4.2 we derive an equation to plot the phase of a spin system. Finally in sec 4.3 we drive the spin-1 system to study its synchronization properties.

4.1 Spin as a Self-Sustained Oscillator

A spin could be modeled as a quantum SSO with a natural description of phase given by spin coherent states $|\theta, \phi\rangle$ [27]. For a spin-s system, $|\theta, \phi\rangle$ is defined by rotating the maximal state $|s, m = s\rangle$

$$|\theta, \phi\rangle = \exp(-i\phi S_z) \exp(-i\theta S_y)|s, s\rangle \ . \tag{4.1}$$

where the spin operators are generators of the rotation group SO(3) satisfying $[S_j, S_k] = i\epsilon_{jkl} S_l$. The range of θ is $[0, \pi]$, whereas the range of ϕ is $[0, 2\pi)$. Similar to a

coherent state for a harmonic oscillator, a spin coherent state is the state closest to a classical spin [28] with an orientation of (θ, ϕ) in spherical coordinates. Using the Wigner-D matrix [29] these states could be written as:

$$\begin{aligned} |\theta, \phi\rangle &= \sum_{m=-s}^{s} \binom{2s}{s+m}^{\frac{1}{2}} \cos^{s+m}\left(\frac{\theta}{2}\right) \sin^{s-m}\left(\frac{\theta}{2}\right) e^{-im\phi}|s, m\rangle \\ &= \sum_{m=-s}^{s} N_{s,m}(\theta) e^{-im\phi}|s, m\rangle \ , \end{aligned} \tag{4.2}$$

where $N_{s,m}(\theta)$ is given by

$$N_{s,m}(\theta) = \binom{2s}{s+m}^{\frac{1}{2}} \cos^{s+m}\left(\frac{\theta}{2}\right) \sin^{s-m}\left(\frac{\theta}{2}\right). \tag{4.3}$$

Additionally, for a spin-1 system the coherent states in Eq 4.2 take the following form

$$|\theta, \phi\rangle = \cos^2\left(\frac{\theta}{2}\right) e^{i\phi}\,|1, 1\rangle + \sqrt{2}\cos\left(\frac{\theta}{2}\right) \sin\left(\frac{\theta}{2}\right)|1, 0\rangle + \sin^2\left(\frac{\theta}{2}\right) e^{-i\phi}\,|1, -1\rangle \tag{4.4}$$

The time evolution of $|\theta, \phi\rangle$ under the free hamiltonian $H = \omega_0 S_z$ is given by $\exp(-iH_0 t)|\theta, \phi\rangle = |\theta, \phi + \omega_0 t\rangle$ [30]. ϕ naturally undergoes rotation under the free hamiltonian and could be treated as a phase variable. Moreover, we could see in Eq 4.2 that ϕ determines the relative phase between basis states whereas θ determines the population.

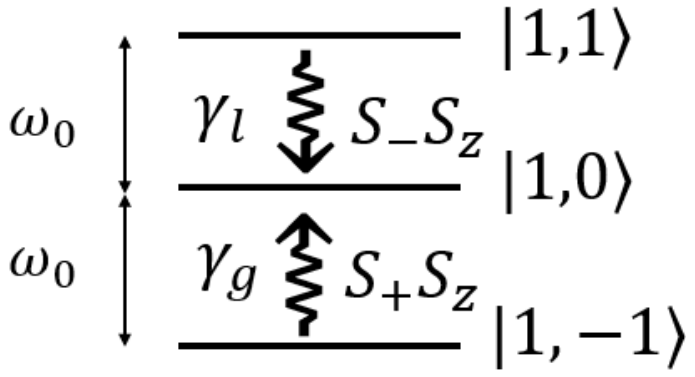

Figure 4.1: A self-sustained oscillator modeled with a spin-1 system. The Lindblad dissipators cause only two types of transitions, from state $|1, 1\rangle$ and $|1, -1\rangle$ to $|1, 0\rangle$, with rates γ_l and γ_g. Basically all initial states are stabilized to $|1, 0\rangle$, this gives us a limit-cycle behavior with steady-state $|1, 0\rangle$.

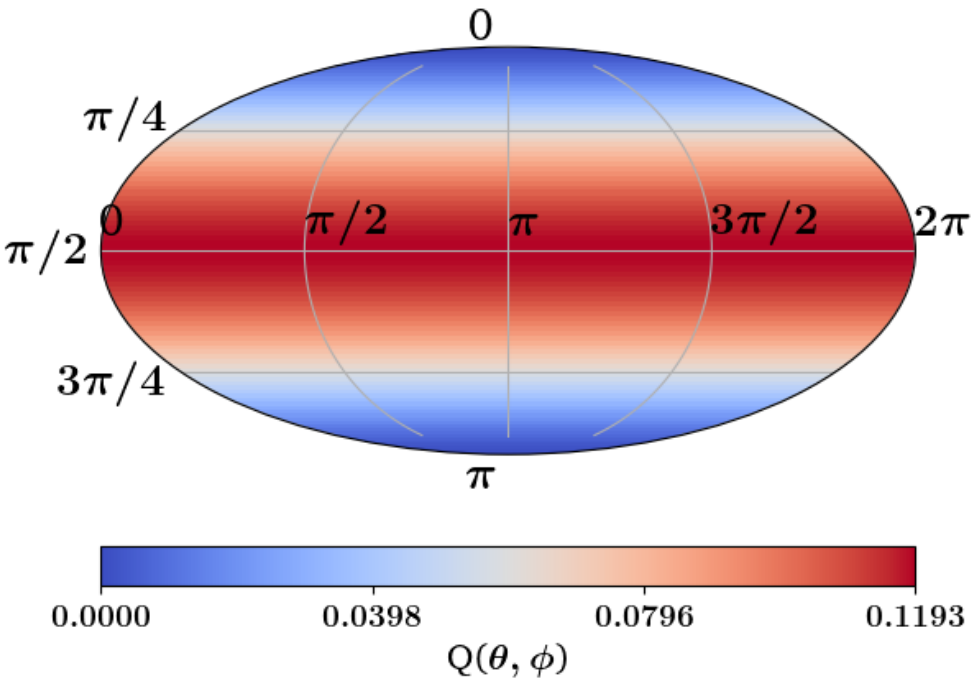

Figure 4.2: The steady state of Eq 4.19 is $|1,0\rangle$ for any non-zero γ_l and γ_g, the Q function for this state is distributed symmetrically about ϕ on the equator. The figure shows the Winkel Tripel projection of the Q-function sphere, with a free phase ϕ on the equator.

A standard SSO model to study synchronization in spin systems is a Spin-1 atom with an equatorial limit cycle [30]. The Lindblad master equation for this oscillator is,

$$\dot{\rho} = -i[H_0, \rho] + \gamma_g \mathcal{D}[S_+ S_z]\rho + \gamma_l \mathcal{D}[S_- S_z]\rho, \tag{4.5}$$

where $H_0 = \omega_0 S_z$, with γ_g and γ_l being the gain and loss rates. We define $\alpha = \gamma_g/\gamma_l$, the gain-to-loss ratio for a spin-1 limit cycle. The Lindbladian dissipators stabilize the spin-1 system to $|1,0\rangle$ state.

To observe the free phase of this system, we plot its Huisimi Q-function using the spin coherent states. The Huisimi Q-Function for spin-s is defined as [31]

$$Q(\theta,\phi) = \frac{2s+1}{4\pi}\langle\theta,\phi|\rho|\theta,\phi\rangle \ . \tag{4.6}$$

With the range of θ and ϕ being $[0,\pi]$ and $[0,2\pi)$ respectively, we could visualize the Q-function over a sphere with each point it being parametrized by (θ,ϕ), similar to cartesian

coordinates. To visualize a sphere on a flat surface we can use the Winkel Tripel Projection [32]. The Q-distribution for the steady state of Eq 4.19, i.e. $|1,0\rangle$, forms an equatorial limit cycle and as we could see from fig 4.2, this limit cycle is evenly spread out in ϕ from 0 to π. This shows that the system has a free phase ϕ and forms a valid SSO.

4.2 Phase Distribution for a Spin

The information about the phase of a spin could be extracted from its phase space distribution in (θ, ϕ), similar to the case of a harmonic oscillator. We use the Q-function for a spin, as defined in Eq 4.6, to find the phase distribution. As ϕ is the phase of interest for the spin system whereas θ just determines the population, we integrate out θ to obtain the distribution $P(\phi)$ as follows

$$\begin{aligned} P_q(\phi) &= \int_0^\pi d\theta \sin(\theta) Q(\theta,\phi) \\ &= \frac{2s+1}{4\pi} \int_0^\pi d\theta \sin(\theta) \langle\theta,\phi|\rho|\theta,\phi\rangle, \end{aligned} \tag{4.7}$$

expanding the density matrix in the above equation in $\{|s,m\rangle\}$ basis we get

$$\begin{aligned} P_q(\phi) &= \frac{2s+1}{4\pi} \sum_{mn} \langle s,m|\,\rho\,|s,n\rangle \int_0^\pi d\theta \sin(\theta) \langle\theta,\phi\,|s,m\rangle\,\langle s,n|\,\theta,\phi\rangle \\ &= \frac{2s+1}{4\pi} \sum_{mn} \langle s,m|\,\rho\,|s,n\rangle \int_0^\pi d\theta \sin(\theta) N_{s,m}(\theta) N_{s,n}(\theta) \exp\{i(m-n)\phi\} \\ &= \frac{2s+1}{4\pi} \sum_{mn} \langle s,m|\,\rho\,|s,n\rangle\, T_q(m,n) \exp\{i(m-n)\phi\} \\ &= \frac{1}{2\pi} + \frac{2s+1}{4\pi} \sum_{m\neq n} \langle s,m|\,\rho\,|s,n\rangle\, T_q(m,n) \exp\{i(m-n)\phi\}, \end{aligned} \tag{4.8}$$

where $T_q(m,n)$ is the integral of the θ part and is defined as

$$T_q(m,n) = \int_0^\pi d\theta \sin(\theta) N_{s,m}(\theta) N_{s,n}(\theta), \tag{4.9}$$

with properties $T_q(m,m) = 2/(2s+1)$ and $T_q(m,n) = T_q(n,m)$. As we can see from Eq 4.8, a diagonal state in the basis $|s,m\rangle$ has a uniform phase distribution. For the existence of

phase selectivity in the spin system it is necessary to have coherences.

We define a new term C_k^q as follows

$$C_k^q = \sum_{m-n=k} \langle m| \rho |n\rangle \, T_q(m,n), \tag{4.10}$$

it could be decomposed into its angular and radial part as $C_k^q = A_k^q \exp(i\Theta_q^k)$, using this definition Eq 4.8 could be further expanded as

$$\begin{aligned}
P_q(\phi) &= \frac{1}{2\pi} + \frac{2s+1}{4\pi} \sum_{m\neq n} \langle s,m| \rho |s,n\rangle \, T_q(m,n) \exp\{i(m-n)\phi\} \\
&= \frac{1}{2\pi} + \frac{2s+1}{4\pi} \sum_{m>n} \langle s,m|\rho|s,n\rangle T_q(m,n) \;\; \exp\{i(m-n)\phi\} + \langle s,n|\rho|s,m\rangle T_q(n,m) \;\; \exp\{i(n-m)\phi\} \\
&= \frac{1}{2\pi} + \frac{2s+1}{4\pi} \sum_{k=1}^{2s} \left[\exp(ik\phi) \sum_{m-n=k} \langle s,m| \rho |s,n\rangle \, T_q(m,n) \right] + h.c. \\
&= \frac{1}{2\pi} + \frac{2s+1}{4\pi} \sum_{k=1}^{2s} [C_k^q \exp(ik\phi)] + h.c. \\
&= \frac{1}{2\pi} + \frac{2s+1}{4\pi} \sum_{k=1}^{2s} [A_k^q \exp\{i(k\phi + \Theta_k^q)\}] + h.c. \\
&= \frac{1}{2\pi} + \frac{2s+1}{2\pi} \sum_{k=1}^{2s} A_k^q \cos(k\phi + \Theta_k^q) \; .
\end{aligned} \tag{4.11}$$

Similar to the case of the harmonic oscillator, the phase distribution has been reduced to a superposition of different harmonic modes. All the off-diagonal density matrix elements which contribute to phase locking, form a set S, these elements could be further divided into subsets S_k with elements $\langle s, m+k| \rho |s,m\rangle$. The elements of S_k contribute to the k-th mode of the distribution. The subset S_k with the largest A_q^k is the dominant subset, we label it as k_d. This means that k_d harmonic mode dominates the phase distribution and its major features will be determined by $\cos(k_d\phi + \Theta_{k_d}^w)$. The distribution will have k_d peaks between 0 to 2π, with the location given by $\phi_p = (2n\pi - \theta)/k$, where n is an integer.

Similar to the case of a harmonic oscillator we could also use states with defined phases to find the phase distribution. For a spin when we talk about phase ϕ, in the classical sense this is the angle subtended by spin vector $\hat{\mathbf{S}}$ on the x-y plane. Studies on the phase operator $\hat{\phi}$ for a spin and its exponential $e^{i\hat{\phi}}$ have been done [33]. For a spin-s system, eigenvalues for

the phase operator $\hat{\phi}$ are given by

$$|\phi_n\rangle = \frac{1}{\sqrt{2s+1}} \sum_{m=-s}^{s} e^{-im\phi_n} |s,m\rangle. \tag{4.12}$$

The phase eigenvalues $\{\phi_n\}$ for a spin are discretized, with $\phi_n = \frac{2n\pi}{2s+1}$. In the classical limit for the spin when $s \to \infty$, $\{\phi_n\}$ becomes continuous over $(0, 2\pi)$. The $(2s+1)$ phase eigenstates $\{|\phi_n\rangle\}$ form a complete orthonormal basis for the spin Hilbert space. To get a continuous distribution over the phase, similar to the case of quasiprobability distribution, we allow ϕ_n to take continuous values over the range $(0, 2\pi)$. Now a phase state $|\phi\rangle$ is given by

$$|\phi\rangle = \frac{1}{\sqrt{2s+1}} \sum_{m=-s}^{s} e^{-im\phi} |s,m\rangle, \tag{4.13}$$

where ϕ could take any value. The states $\{|\phi\rangle\}$ now form an overcomplete basis for the Hilbert space, similar to the spin coherent states, yielding a resolution to unity

$$\frac{2s+1}{2\pi} \int_0^{2\pi} d\phi \; |\phi\rangle \langle\phi| = 1 \; . \tag{4.14}$$

The phase distribution for a single spin s using phase states is given by

$$P_p(\phi) = \frac{2s+1}{2\pi} \langle\phi| \rho |\phi\rangle \, , \tag{4.15}$$

simplifying the above equation, it could be simplified to a form similar to Eq 4.11. We define a new term C_k^p as follows

$$C_k^p = \sum_{m-n=k} \langle m| \rho |n\rangle \, , \tag{4.16}$$

it could be decomposed into its angular and radial part as $C_k^p = A_k^p \exp(i\Theta_p^k)$, the final form of the phase distribution could be written as

$$P_p(\phi) = \frac{1}{2\pi} + \frac{2s+1}{2\pi} \sum_{k=1}^{2s} A_k^p \cos(k\phi + \Theta_k^p). \tag{4.17}$$

The phase distribution derived from phase states is just dependent on density matrix elements unlike Eq 4.11 which is derived from spin's phase space. This helps us to determine the dependence of phase on density matrix elements, similar to Eq 2.33 for the case of a

single quantum harmonic oscillator derived from the phase eigenstates of the SG operator.

4.3 Spin with an external drive

We established a method to plot the phase of a spin and also modeled an SSO using a spin system. Now if we apply an external drive to the spin SSO, we expect to see phase-locking behavior similar to a QVdP. The hamiltonian for an external drive acting on a spin system is given by

$$H_d = i\epsilon \left(e^{i\omega t} S_- - e^{-i\omega t} S_+\right), \tag{4.18}$$

where ϵ is the strength of the drive and ω is its frequency. The master equation for a driven spin-1 SSO becomes

$$\dot{\tilde{\rho}} = -i[\omega_0 S_z + i\epsilon \left(e^{i\omega t} S_- - e^{-i\omega t} S_+\right), \tilde{\rho}] + \gamma_g \mathcal{D}[S_+ S_z]\tilde{\rho} + \gamma_l \mathcal{D}[S_- S_z]\tilde{\rho}. \tag{4.19}$$

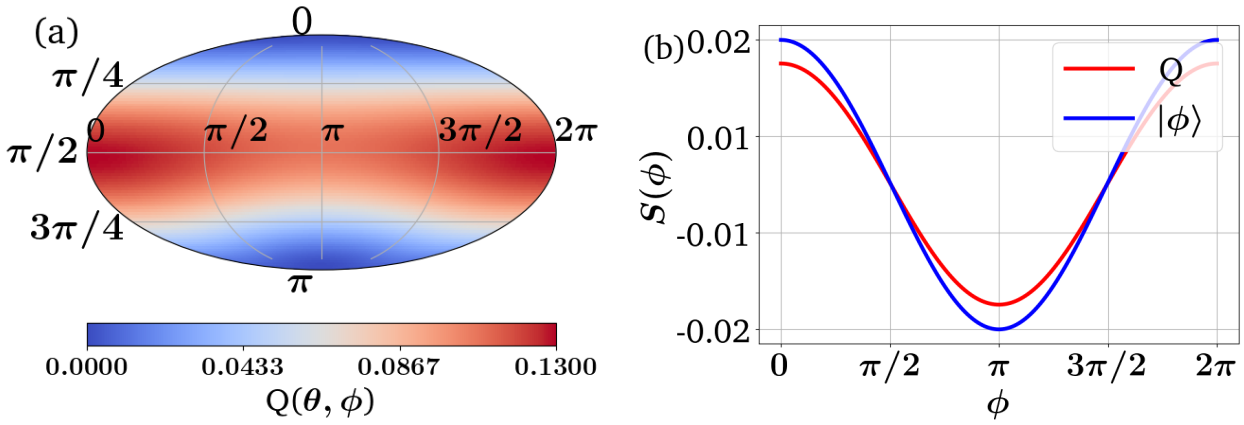

Figure 4.3: Driving a spin-1 system with equatorial limit cycle results in phase localization at a certain value of ϕ. Here the rates for the dissipators have the ratio $\gamma_g/\gamma_l = 0.1$ with $\epsilon = 0.1\gamma_g$. (a)The system no more has a uniformly distributed Q-function about the equator as in fig 4.2, the distribution becomes localized about $\phi = 0$,(b)Phase distribution for the driven spin derived from its Q-distribution (red) and phase states $|\phi\rangle$ (blue), here also we could see that the phase is peaked about $\phi = 0$.

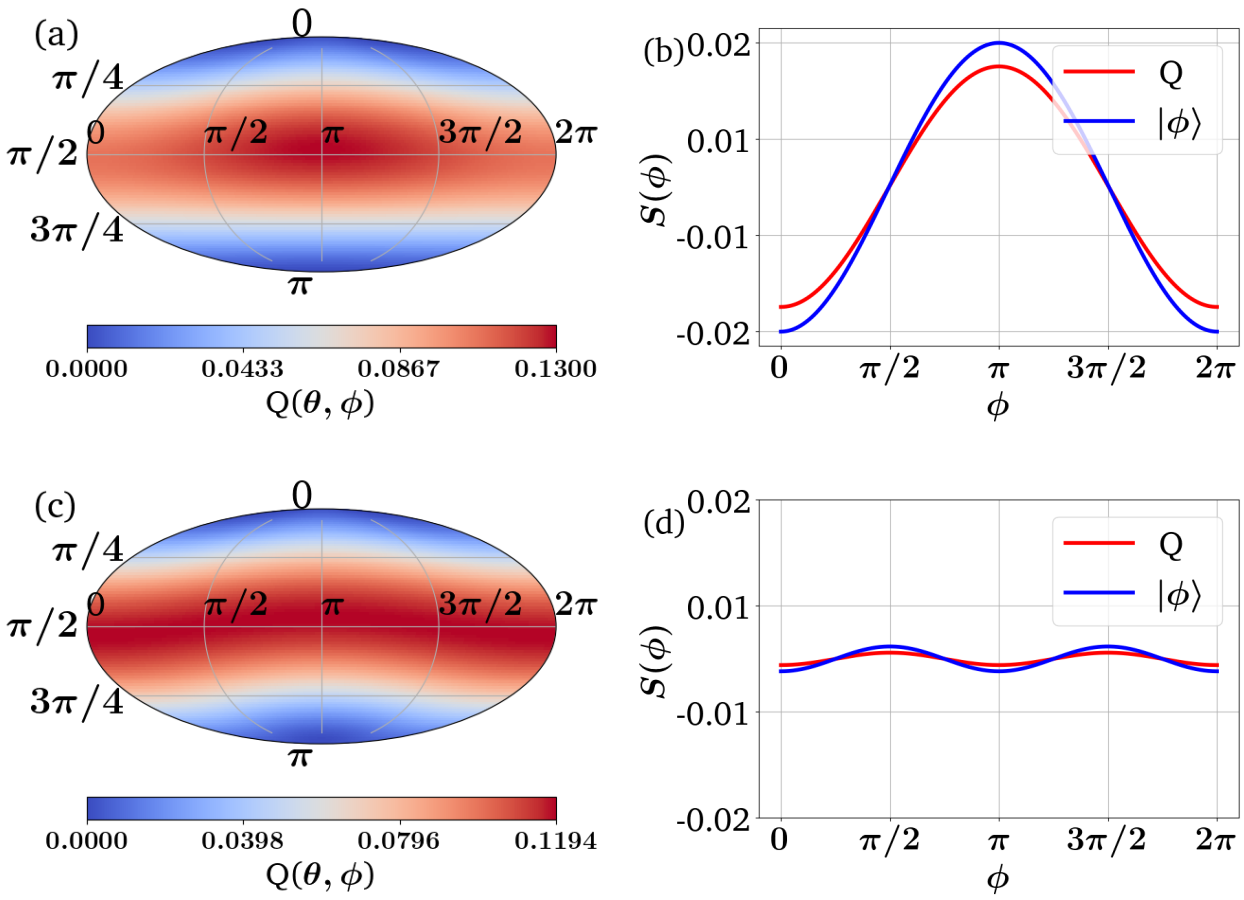

Figure 4.4: The ratio of gain and loss rates γ_l/γ_g for the spin-1 oscillator is significant in determining the nature of synchronization after application of drive. In fig 4.3 we saw that relative phase peaks at $\phi = 0$ for $\gamma_g/\gamma_l = 0.1$. For $\Delta = 0$ and $\epsilon = 0.1\min\{\gamma_g, \gamma_l\}$, fig (a) and (b) shows the Winkel Tripel Projection of the Q-function and relative phase distribution for parameters $\gamma_g/\gamma_l = 10$, here we can see that the relative phase is peaked about $\phi = \pi$. Whereas (c) and (d) are for the parameters $\gamma_g/\gamma_l = 1$, here we could see that the relative phase doesn't show a strong locking similar to other cases.

As we want to study the phase locking of the spin with an external drive, we move into the drive's frame with the following unitary transform

$$\rho = \exp\left(i\omega_0 S_z\right)\tilde{\rho}\exp\left(-i\omega_0 S_z\right) , \tag{4.20}$$

the master equation in the drive's frame is given by [30]

$$\dot{\rho} = -i[\Delta S_z + \epsilon S_y, \rho] + \gamma_g \mathcal{D}[S_+ S_z]\rho + \gamma_l \mathcal{D}[S_- S_z]\rho, \tag{4.21}$$

where Δ is the detuning between the natural frequency of the oscillator and the drive. Application of the drive leads to phase localization, as we could see from fig 4.3 when we apply a drive of amplitude $\epsilon = 0.1\gamma_g$ with the dissipators' rates having the ratio $\gamma_g/\gamma_l = 0.1$, the phase is localized about the point $\phi = 0$. This confirms that a finite-dimensional purely quantum system could also show synchronization.

The ratio of gain and loss rates α has a significant influence over the synchronization properties of the spin. As we can see from fig 4.3 and 4.4, the spin system is able to synchronize to an external drive only when the rates for the dissipators are unbalanced, i.e. either the gain is dominant or the loss is dominant. For balanced dissipators such that $\gamma_l = \gamma_g$, we don't observe any synchronization [30], the phase is still uniformly distributed about the equator.

Chapter 5

Synchronization between Two Spins

In chapter 4 we saw how we could model a spin as a self-sustained oscillator and synchronize it to an external drive. Similar to the case of two QHO in chapter 3, we could also synchronize two spins by introducing relevant coupling between them.

The master equation for two spin-1 systems with an equatorial limit cycle is given by

$$\dot{\rho} = -i\left[\sum_{i=1,2}\omega_i S_z^{(i)}, \rho\right] + \sum_{i=1,2}\gamma_g^{(i)}\mathcal{D}[S_+^{(i)}S_z^{(i)}]\rho + \gamma_l^{(i)}\mathcal{D}[S_-^{(i)}S_z^{(i)}]\rho, \tag{5.1}$$

where $\omega_i, \gamma_g^{(i)}$ and $\gamma_l^{(i)}$ are the same parameters as defined in sec 4.1 for i-th spin. The density matrix for uncoupled spins could be simply written as a tensor product for two states, $\rho = \rho_1 \otimes \rho_2$. As the steady state for a single spin-1 oscillator is $|1,0\rangle$, the steady state for Eq 5.1 is $|1,0;1,0\rangle$. Now we need to apply a suitable coupling between the spins to synchronize them and investigate their joint phase space for extracting the relative phase information.

The chapter is organized as follows, in sec 5.1 we use the joint phase space distribution for two spins to plot the relative phase distribution, and in sec 5.2 we introduce a coherent coupling between the spins to study their synchronization behavior.

5.1 Relative Phase Distribution of Two Spins

To calculate the relative phase distribution between two spins we use the two-mode Huisimi Q [34] function as it completely captures all correlations that could exist between two spins. For spins s_1 and s_2, the two-mode Q function for the joint state ρ is defined as

$$Q(\theta_1, \phi_1, \theta_2, \phi_2) = \frac{(2s_1+1)(2s_2+1)}{(4\pi)^2} \langle \theta_1, \phi_1; \theta_2, \phi_2 | \rho | \theta_2, \phi_2; \theta_1, \phi_1 \rangle, \tag{5.2}$$

where $|\theta_i, \phi_i\rangle$ is the spin coherent state for i-th spin. Expanding ρ in the joint basis $\{|s_1, m_1; s_2, m_2\rangle\}$ we get:

$$Q = \frac{(2s_1+1)(2s_2+1)}{(4\pi)^2} \sum_{m_1,m_2,n_1,n_2} \langle s_1, m_1; s_2, m_2 | \, \rho \, | s_1, n_1; s_2, n_2 \rangle$$
$$\langle \theta_1, \phi_1; \theta_2, \phi_2 | \, s_1, m_1; s_2, m_2 \rangle \langle s_1, n_1; s_2, n_2 \, | \theta_1, \phi_1; \theta_2, \phi_2 \rangle$$

$$= \frac{(2s_1+1)(2s_2+1)}{(4\pi)^2} \sum_{m_1,m_2,n_1,n_2} \langle s_1, m_1, ; s_2, m_2 | \, \rho \, | s_1, n_1; s_2, n_2 \rangle \, N_{s_1,m_1}(\theta_1) N_{s_2,m_2}(\theta_2) N_{s_1,n_1}(\theta_1) N_{s_2,n_2}(\theta_2)$$
$$\exp\{i(m_1 - n_1)\phi_1\} \exp\{i(m_2 - n_2)\phi_2\} \tag{5.3}$$

To study phase locking we will have to extract the information about the relative phase, i.e. $\phi = (\phi_1 - \phi_2)$, from the joint Q distribution. To do this we transform the variables of the joint Q function from $(\theta_1, \theta_2, \phi_1, \phi_2)$ to $(\theta_1, \theta_2, \phi, \kappa)$, where $\kappa = (\phi_1 + \phi_2)$, and then we integrate out θ_1, θ_2 and κ to get a distribution in ϕ, i.e. $P_q(\phi)$.

$$P_q(\phi) = \int_0^{\pi} d\theta_1 \sin(\theta_1) \int_0^{\pi} d\theta_2 \sin(\theta_2) \int_0^{4\pi} d\kappa \, \frac{1}{2} Q(\theta_1, \theta_2, \kappa, \phi) \tag{5.4}$$

Plugging in the explicit equation for the Q function in 5.3 we get

$$P_q(\phi) = \frac{(2s_1+1)(2s_2+1)}{(4\pi)^2} \sum_{m_1,m_2,n_1,n_2} \langle s_1, m_1; s_2, m_2 | \, \rho \, | s_1, n_1; s_2, n_2 \rangle \exp\{i/2 \left[(m_1 - n_1) - (m_2 - n_2)\right] \phi\}$$
$$\int_0^{\pi} d\theta_1 \sin(\theta_1) N_{s_1,m_1}(\theta_1) N_{s_1,n_1}(\theta_1) \int_0^{\pi} d\theta_2 \sin(\theta_2) N_{s_2,m_2}(\theta_2) N_{s_2,n_2}(\theta_2) \times$$
$$\int_0^{4\pi} d\kappa \, \frac{1}{2} \exp\{i/2 \left[(m_1 + m_2) - (n_1 + n_2)\right] \kappa\} \tag{5.5}$$

Similar to the case of relative phase distribution for two harmonic oscillators, the integral over κ eliminates those density matrix terms that don't satisfy $(m_1 + m_2 \neq n_1 + n_2)$. This gives us a similar selection rule as in the case of phase locking between two harmonic oscillators, i.e. relative phase between two spins is determined by those joint density matrix elements $\langle s_1, m_1; s_2, m_2| \rho |s_1, n_1; s_2, n_2\rangle$ which satisfy:

$$m_1 + m_2 = n_1 + n_2 \tag{5.6}$$

Simplifying the equation further we get

$$\begin{aligned} P(\phi) &= \frac{(2s_1+1)(2s_2+1)}{8\pi} \sum_{m_1+m_2=n_1+n_2} \langle s_1, m_1; s_2, m_2| \rho |s_1, n_1; s_2, n_2\rangle \times \\ &\qquad I_q(m_1, m_2, n_1, n_2) \exp\{i(m_1 - n_1)\phi\} \\ &= \frac{1}{2\pi} + \frac{(2s_1+1)(2s_2+1)}{8\pi} \sum_{\substack{m_1+m_2=n_1+n_2 \\ m_1 \neq n_1}} \langle s_1, m_1; s_2, m_2| \rho |s_1, n_1; s_2, n_2\rangle \times \\ &\qquad I_q(m_1, m_2, n_1, n_2) \exp\{i(m_1 - n_1)\phi\} \end{aligned} \tag{5.7}$$

where $I_q(m_1, m_2, n_1, n_2) = T_q(m_1, n_1)T_q(m_2, n_2)$. Eq 5.7 tells us that the relative phase distribution for a state diagonal in the joint basis $|s_1, m_1; s_2, m_2\rangle$ is uniform with no phase locking. For phase locking to exist we require off-diagonal coherence terms that follow the selection rule in Eq 5.6.

We define a new term C_k^q as follows

$$C_k^q = \sum_{m_1 - n_1 = k} \langle s_1, m_1; s_2, m_2| \rho |s_1, n_1; s_2, n_2\rangle \, I_q(m_1, m_2, n_1, n_2), \tag{5.8}$$

it could be decomposed into its angular and radial part as $C_k^q = A_k^q \exp(i\Theta_q^k)$. The relative phase distribution in Eq 5.6 could be reduced to a superposition of different harmonic modes as follows

$$P_q(\phi) = \frac{1}{2\pi} + \frac{(2s_1+1)(2s_2+1)}{4\pi} \sum_{k=1}^{2s_1} A_k^q \cos(k\phi + \Theta_k^q) \ . \tag{5.9}$$

The elements following the selection rule in Eq 5.6, which contribute to the relative phase distribution form a set S, this set could be further divided into subsets S_k based on the classification $\langle s_1, m_1 + k; s_2, m_2| \rho |s_1, m_1; s_2, m_2 + k\rangle$. Elements of the subset S_k contribute to the k-th harmonic of the relative phase distribution.

We could also use the phase states $\{|\phi\rangle\}$ for spin systems as defined in Eq 4.13. For a system of two spins, s_1 and s_2 the joint phase distribution is given by:

$$P(\phi_1, \phi_2) = \frac{(2s_1+1)(2s_2+1)}{(2\pi)^2} \langle \phi_1, \phi_2 | \rho | \phi_1, \phi_2 \rangle . \tag{5.10}$$

Similar to previous case in Eq 5.5, transforming the variables ϕ_1 and ϕ_2 to ϕ and κ, then integrating over κ to get $P(\phi)$, we obtain the same selection rule as in Eq 5.6. We define a new term C_k^p as follows

$$C_k^p = \sum_{m_1 - n_1 = k} \langle s_1, m_1; s_2, m_2 | \rho | s_1, n_1; s_2, n_2 \rangle , \tag{5.11}$$

it could be decomposed into its angular and radial part as $C_k^p = A_k^p \exp(i\Theta_k^p)$ The relative phase distribution obtained from phase states could be simplified to a form similar to Eq 5.12 as follows

$$P_p(\phi) = \frac{1}{2\pi} + \frac{(2s_1+1)(2s_2+1)}{4\pi} \sum_{k=1}^{2s_1} A_k^p \cos(k\phi + \Theta_k^p) . \tag{5.12}$$

This relative phase distribution derived from phase state is only dependent on density matrix elements unlike the one derived from phase space distribution which is also dependent on theta integrals. This helps us clearly determine the dependence of relative phase between two oscillators, on their joint density matrix elements.

5.2 Synchronizing Interactions

Now after we have modeled a system of two spin oscillators and established a method to plot its relative phase distribution, we need to introduce relevant interactions between them to phase lock the oscillators. One of the standard forms of couplings that we could introduce between two spins is coherent exchange interaction with hamiltonian of the following form

$$H_c = i\gamma_c \left(S_1^+ S_2^- - S_2^+ S_1^- \right) \tag{5.13}$$

where S_i^+ and S_i^- are the raising and lowering operators for i-th spin, with γ_c being the strength of coupling. The complete master equation for two coherently coupled spins with

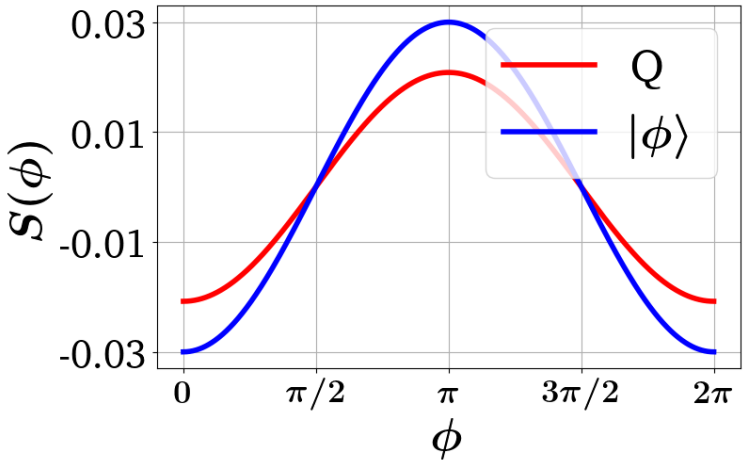

Figure 5.1: Coherent coupling of the from $i\gamma_c \left(S_1^+ S_2^- - S_2^+ S_1^-\right)$ leads to phase locking between the spins, as could be seen from the non-uniform phase distributions. The phase distributions are calculated from the Q function (red) and phase states $\{|\phi\rangle\}$ (blue). The parameters for the system are $\gamma_g^{(1)} = \gamma_l^{(2)} = 1, \gamma_l^{(1)} = \gamma_g^{(2)} = 100, \omega_1 = \omega_2 = 1$ and $\gamma_c = 0.1$. This coupling generates coherences in the steady state which follow the selection rule in Eq 5.6.

an equatorial limit cycle is given by

$$\dot{\rho} = -i\left[\sum_{i=1,2} \omega_i S_z^{(i)} + i\gamma_c \left(S_1^+ S_2^- - S_2^+ S_1^-\right), \rho\right] + \sum_{i=1,2} \gamma_g^{(i)} \mathcal{D}[S_+^{(i)} S_z^{(i)}]\rho + \gamma_l^{(i)} \mathcal{D}[S_-^{(i)} S_z^{(i)}]\rho, \quad (5.14)$$

The coherent interaction leads to phase locking between the two spins [34], this is seen from the non-uniform relative phase distribution between the two spins, as in fig 5.1. This is because the coupling generates coherences as per selection rule Eq 5.6, this could be seen from fig 5.2. Moreover, as the distribution produced has a single peak between 0 and 2π, the dominant subset in the steady state density matrix is S_1, as shown in fig 5.2.

The ratio of gain and loss rates for the spin has a significant effect on the phase-locking behavior. As we can see from fig 5.1 and 5.3, the spins show strong phase locking when the ratio of gain and loss rates is unbalanced. Whereas for a balanced case, the relative phase distribution becomes nearly flat with an evenly distributed phase [34].

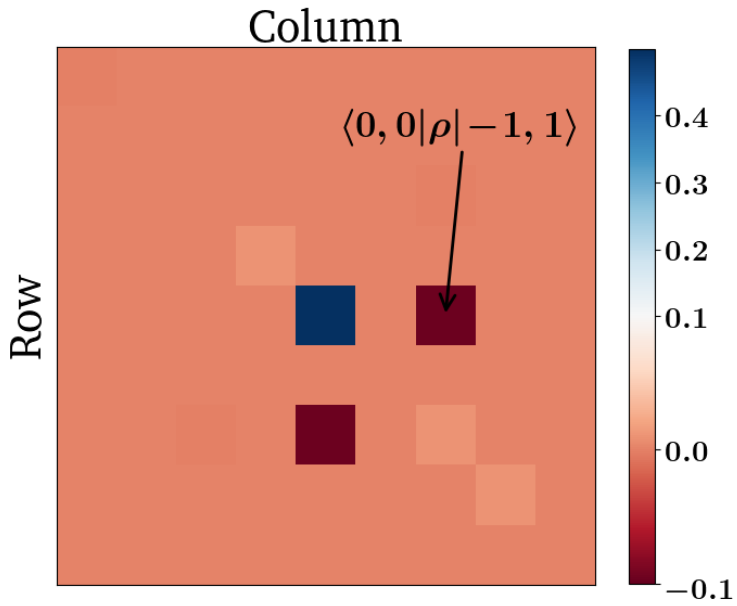

Figure 5.2: Coherent coupling leads to an unimodal peak in the relative phase distribution, this tells us that selection rule elements are being generated because of it and more specifically elements from the subset S_1. In the figure we have the color plot for the steady state density matrix of Eq 5.14 with the parameters for the system are $\gamma_g^{(1)} = \gamma_l^{(2)} = 1, \gamma_l^{(1)} = \gamma_g^{(2)} = 100, \omega_1 = \omega_2 = 1$ and $\gamma_c = 0.1$. As we can see the major coherence term is $\langle 0, 0| \rho |-1, 1\rangle$, which belongs to the S_1 subset, with the contribution of $\cos(\phi)$.

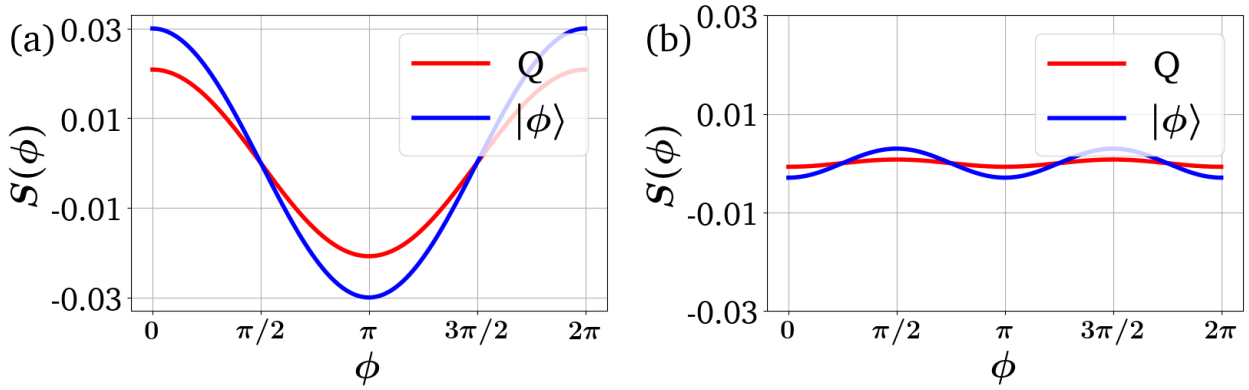

Figure 5.3: The gain and loss rates control the phase locking between the spins. For $\omega_1 = \omega_2 = 1$ and $\gamma_c = 0.1$ we have (a)$\gamma_g^{(1)} = \gamma_l^{(2)} = 100, \gamma_l^{(1)} = \gamma_g^{(2)} = 1$, here we have a similar limit cycle as fig 5.1 but with reversed rates which shifts the peak from π to 0, and (b)$\gamma_g^{(1)} = \gamma_l^{(2)} = \gamma_l^{(1)} = \gamma_g^{(2)} = 1$, here we have a ration of gain and loss rates for the spins is equal, for this case the synchronization is greatly reduced with a nearly flat distribution.

Chapter 6

Coherences and Correlations

Synchronization has a close connection with coherences as we saw in previous chapters. Whether it is synchronization of a single quantum unit to an external drive or between two quantum systems, synchronization requires the existence of certain coherence terms in the density matrix. This connection between coherence and synchronization has been previously observed in many studies [34, 35, 36]. Moreover, as soon as we move to a bipartite setting, apart from coherences it is also important to consider the existence of correlations between the systems and how they affect the phase-locking behavior. Many studies have explored this question of the relation between synchronization and various forms of correlations, like entanglement and discord [34, 25, 37].In this chapter, we look at various examples of synchronization setups and investigate if there is a one-to-one correspondence between these quantities and synchronization.

6.1 Coherences

As we saw in Eq 2.17, 3.6, 4.8 and 5.7, that existence of coherence is necessary for existence if synchronization. For a single QHO and a single spin, all forms of off-diagonal coherences contributed to phase locking, but for the case of two QHO and two spins only specific kinds of coherences contributed to relative phase distribution determined by the selection rules 3.5 and 5.6.

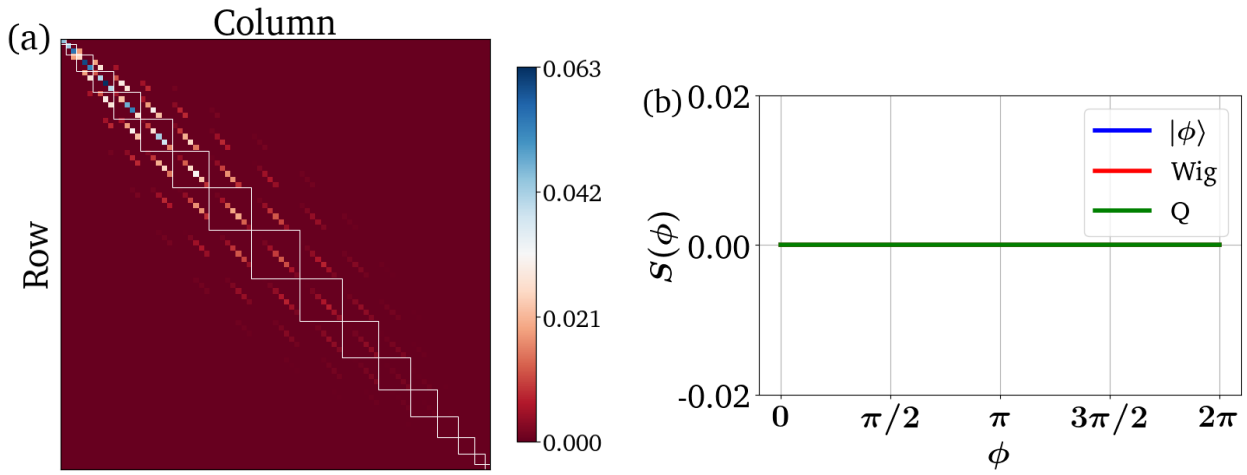

Figure 6.1: Synchronization between two quantum oscillators is a result of selection rule coherences, existence of other coherences doesn't lead to any phase locking. Here we have two dissipatively coupled QVdP with interaction of the form $\gamma_d \mathcal{D}[a_1 + a_2^2]$ and parameters given by $\omega_1 = \omega_2 = 1, \gamma_l^{(1)} = \gamma_l^{(2)} = 0.2, \gamma_g^{(1)} = \gamma_g^{(2)} = 1$ and $\gamma_d = 1$.(a) This is the color plot for the absolute value of steady-state density matrix elements in the joint Fock basis such that states with the same total occupation are grouped together. Here we could see that unlike fig 3.4 and 3.7, the coherences exist outside the conserved total occupation subspaces which doesn't result in any synchronization. (b) $S(\phi)$ for the steady state of the system, as expected the oscillators have a uniform relative phase distribution.

For the case of two oscillators the existence or non-existence of coherences not satisfying the selection rule has no effect on relative phase, two oscillators could have high coherence buildup between them but still no phase locking. This means that simply the existence of coherence doesn't imply synchronization. A generalized measure for bipartite synchronization was proposed in [36], it is based on the distance between a state and the nearest reference limit cycle state of the form

$$\sigma = \sum_i q_i \sigma_i^{(1)} \otimes \sigma_i^{(1)}, \tag{6.1}$$

where $\sigma_i^{(\alpha)}$ is the individual limit cycle state for the oscillators. The measure is defined as

$$S(\rho||\sigma) = \mathrm{Tr}(\rho \ln \rho - \rho \ln \sigma), \tag{6.2}$$

where $S(\rho||\sigma) = \mathrm{Tr}(\rho \ln \rho - \rho \ln \sigma)$. For the case of diagonal limit cycle states, like the one for two uncoupled VdPs, $\Omega_R(\rho)$ reduces to relative entropy of coherence given by

$$S_{coh}(\rho) = S(\rho_{dia} - S(\rho)), \tag{6.3}$$

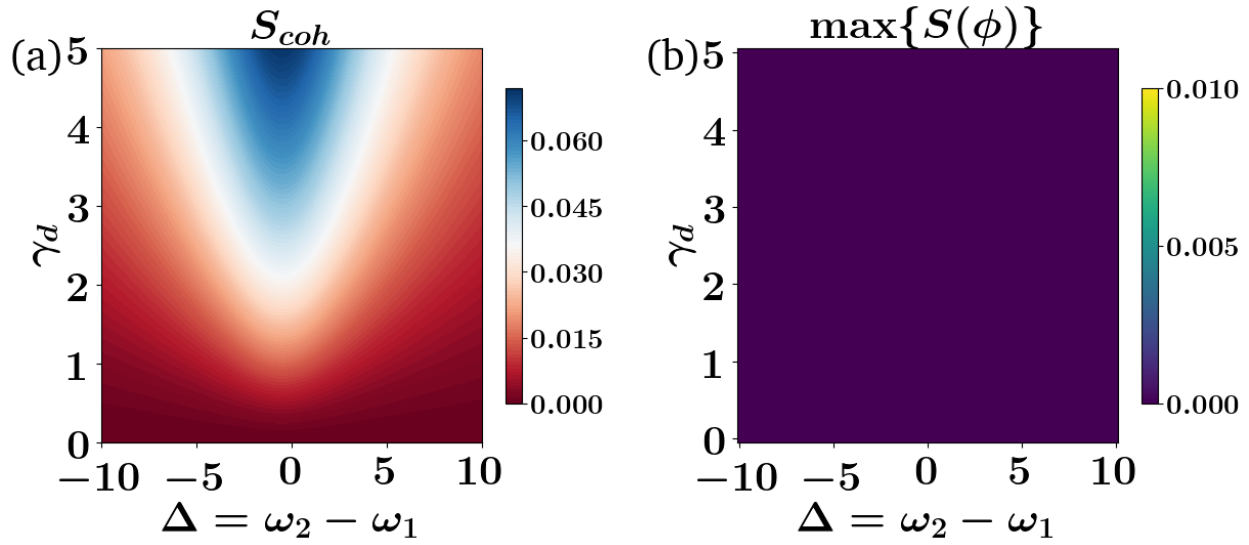

Figure 6.2: Synchronization measures based on coherences, like relative entropy of coherence, are not good measures for the case of bipartite synchronization as these account for all forms of coherences and phase locking of two oscillators is determined by only the selection rule elements. Here we have two dissipatively coupled QVdP with interaction of the form $\gamma_d \mathcal{D}[a_1 + a_2^2]$ and parameters given by $\gamma_l^{(1)} = \gamma_l^{(2)} = 3$ and $\gamma_g^{(1)} = \gamma_g^{(2)} = 1$, we vary the coupling γ_d from 0 to 5 and detuning Δ from -10 to 10. (a) We obtain an Arnold Tongue for relative entropy of coherence S_{coh}, but as we could see from (b) the interaction produces no synchronization at all throughout the whole parameter regime.

where $S(\rho) = -\mathrm{Tr}\{\rho \ln(\rho)\}$ is the Von Neumann entropy and ρ_{dia} is the density matrix obtained by setting all the off-diagonal terms to zero. S_{coh} captures all forms of coherences that could exist between two quantum systems, even those that don't contribute to synchronization. That is why we need to be careful while using various measures and see whether the contributions are coming from coherences as per the selection rule or even the other terms.

Imagine we couple two QVdP dissipatively with a correlated one and two-photon loss of the form $\gamma_d \mathcal{D}[a_1 + a_2^2]$. The uncoupled system has a diagonal limit cycle state, the coupling gives us a steady state that has only those coherences that exist outside the conserved total occupation subspaces, as could be seen in fig 6.1. That is why this form of coupling leads to no synchronization but still, it shows an Arnold tongue behavior in S_{coh}, as could be seen in fig 6.2. To make $\Omega_R(\rho)$ more robust measure for synchronization, in addition to σ we should include all those density matrices in the reference states that have a uniform $P(\phi)$. These states could also be entangled states as will become more clear in the next sec 6.2.

For the case of a single system and a drive, we could safely say that there exists no condition when a system is synchronized to a drive and there are no coherences, but is the existence of coherence a sufficient condition, can there exist scenarios where a system has coherence but no phase locking? The final form of phase distribution for a QHO (Eq 2.33) and a spin (4.7) was reduced to a superposition of harmonic modes with the contribution to each mode being determined by A_k^p, which is basically the absolute value of the sum of all elements in the subset S_k. As we have to sum all the elements in a subset, this makes the relative sign between the elements important as this could result in canceling out of coherences which could make A_k^p close to zero even if the norm of coherence is high. A similar situation could happen for the case of two oscillators where the contribution of selection rule coherences from a subset S_k is in the form of the sum of all coherences which could lead to destructive interference. Examples for this case are in fig 4.4 and 5.3, here the drive and interactions lead to generation of coherences but these coherences interfere destructively to reduce synchronization.

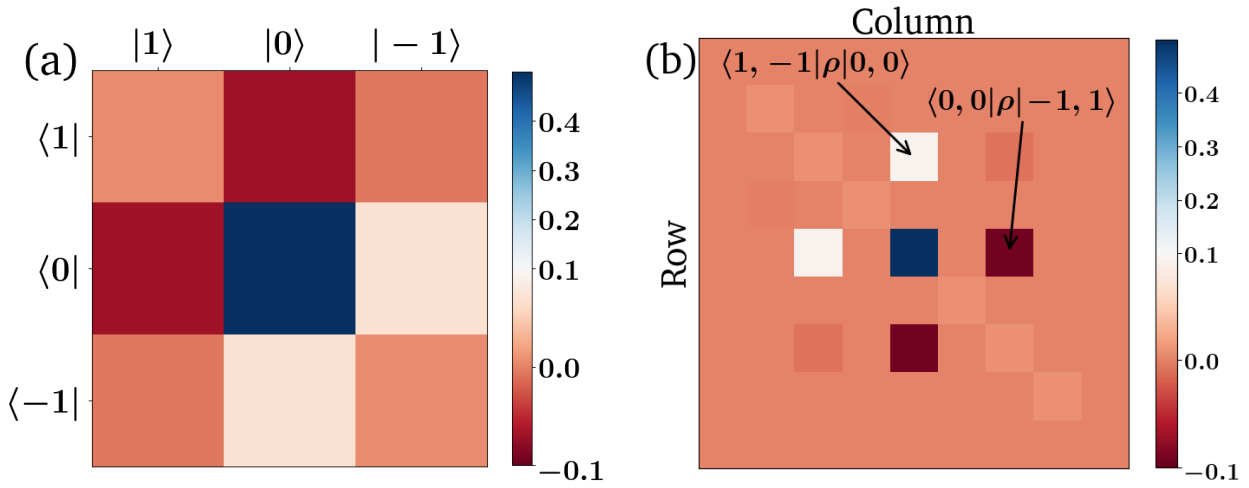

Figure 6.3: Synchronization is a result of the development of coherences in a quantum system, the contribution from a subset S_k is in the form of the sum of all coherences in that subset. This could result in destructive interference of these elements. (a) Color plot for the steady state density matrix of a spin-1 system with master equation 4.21 and parameters $\omega = 1, \epsilon = 0.1$ and $\gamma_l = \gamma_g = 1$. Here we could see that the coherences within the subset S_1 have opposite signs which degrade the phase locking behavior as seen in fig 4.4. (b) Color plot for the steady state density matrix of two spin-1 systems with master equation 5.14 and parameters $\omega_1 = \omega_2 = 1, \gamma_c = 0.1$ and $\gamma_l^{(1)} = \gamma_l^{(2)} = \gamma_g^{(1)} = \gamma_g^{(2)} = 1$. Here we could see that the coherences within the subset S_1 have opposite signs which degrades the phase locking behavior as seen in fig 5.3.

6.2 Correlations

Synchronization of two systems is often accompanied by the development of correlations between them, because of this mutual information was proposed as a measure for synchronization [37]. Given a joint density matrix ρ for two oscillators, mutual information is defined as

$$I(\rho) = S(\rho_1) + S(\rho_2) - S(\rho), \tag{6.4}$$

where $\rho_1 = \mathrm{Tr}_2(\rho)$ and $\rho_2 = \mathrm{Tr}_2(\rho)$. Entanglement is a special form of correlation specific to quantum systems, the relation of synchronization to entanglement has been studied previously in various systems [34, 25]. As per our findings, we saw that synchronization depends on specific density matrix elements, this clearly indicates that not all entangled states would have phase locking. For example in the case of two spin-1 systems, the state $|\psi\rangle = \frac{|1,1\rangle+|0,0\rangle+|-1,-1\rangle}{\sqrt{3}}$ is maximally entangled, but it would have no phase locking as $|\psi\rangle\langle\psi|$ has no coherences as per the selection rule. Whereas the density matrix for state $|\Psi\rangle = \frac{|1,-1\rangle+|0,0\rangle+|-1,1\rangle}{\sqrt{3}}$ has the selection rule elements, that is why it will have non-uniform $P(\phi)$.

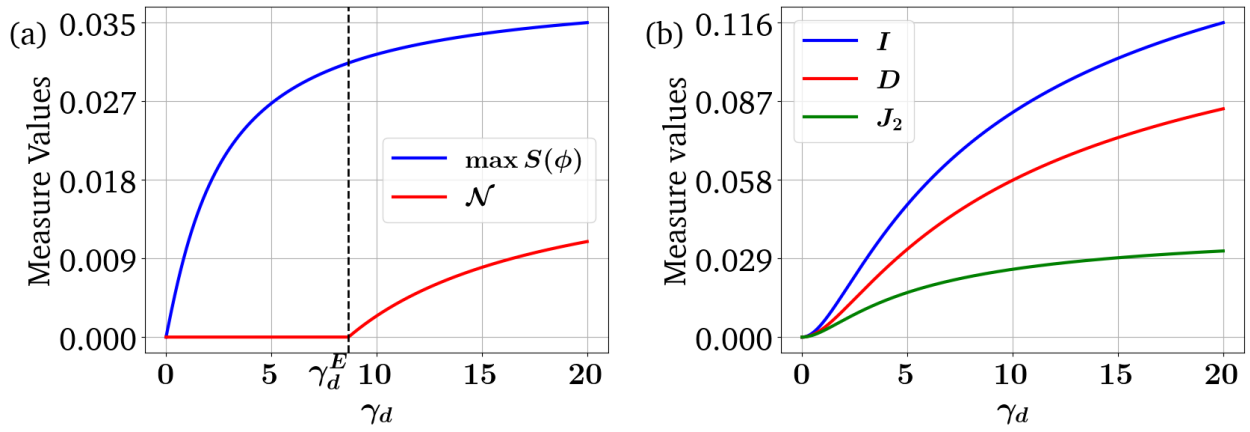

Figure 6.4: Synchronization is not necessarily always accompanied by entanglement, there could exist scenarios when two oscillators are synchronized but not at all entangled. Here we have two QVdP in the dissipative limit coupled with an interaction of the form $\gamma_d\mathcal{D}[a_1 + a_2]$ with $\omega_1 = \omega_2 = 1$ and we vary γ_d from 0 to 20. (a) Synchronization measure $\max\{S(\phi)\}$ starts to increase as soon as γ_d becomes non-zero but negativity $\mathcal{N}$ remains zero till a critical coupling value of γ_d^E. This means that two systems could be synchronized without being entangled. (b) Development of synchronization is accompanied by growth in mutual information I (Blue), which has contributions from both classical information (Green) and quantum discord (Red).

Imagine we have two QVdP in the dissipative limit occupying the lowest two levels and interacting via a correlated one photon loss $\gamma_d \mathcal{D}[a_1 + a_2]$. As negativity is a definite measure of entanglement for two two-level systems [38], it helps us characterize the parameter regime where the QVdP are entangled in the dissipative limit. Negativity is defined as

$$\mathcal{N} = \frac{(\|\hat{\rho}\|_1 - 1)}{2}, \tag{6.5}$$

where $\left\|\hat{\rho}^{T_1}\right\|$ is the trace norm of the partially transposed density matrix over the first VdP. As we can see from fig 6.4 when we increase the coupling, the synchronization measure starts to grow instantly. Whereas negativity remains zero initially, it starts to increase abruptly after a critical value γ_d^E. This shows that there could exist regimes where two systems could have synchronization but no entanglement.

Entanglement is a strong form of quantum correlations, on the other hand, quantum discord captures a wide range of quantum correlations beyond entanglement. Classical information is the maximum amount of information that could be obtained about a system

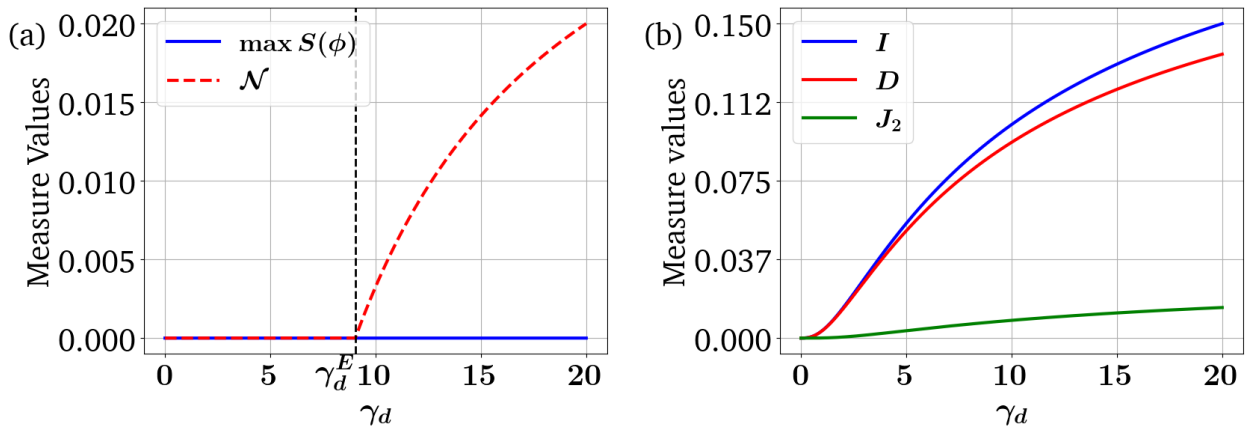

Figure 6.5: Entanglement is also not always accompanied by synchronization, there could exist scenarios when two oscillators are entangled but not at all synchronized. Here we have two QVdP in the dissipative limit coupled with an interaction of the form $\gamma_d \mathcal{D}[a_1^\dagger + a_2]$ with $\omega_1 = \omega_2 = 1$ and we vary γ_d from 0 to 20. (a)Negativity starts to increase after a critical coupling value γ_d^E, the oscillators are entangled for coupling values greater than γ_d^E, but as we can see from the figure the oscillators remain unsynchronized for all coupling values. This shows that there could exist cases when two oscillators are entangled but not at all synchronized. (b) Even without the existence of synchronization mutual information (Blue) grows between the oscillators with contributions from classical information (Green) and quantum discord (Red).

by making measurements on the other system, discord is the difference between total information and the classical information [39]. If we perform the measurements on the second oscillator, this gives us the classical information $J_2(\rho)$ with the discord being

$$D(\rho) = I(\rho) - J_2(\rho) \tag{6.6}$$

The synchronized states of two VdP in the dissipative limit come under the category of X states, i.e. the states with non-zero elements only along the diagonal and anti-diagonal, calculation of discord for these states is straightforward [40]. In fig 6.4 could we see, that as the coupling strength of dissipative interactions increases, mutual information increases between the oscillators. While mutual information has both, classical and quantum contributions, the major weightage is of quantum correlations. This shows that even when two synchronized oscillators are not entangled, there could exist other forms of quantum correlations between them.

Now we know that the existence of synchronization doesn't necessarily imply entanglement, same is true the other way around. If we introduce a new coupling of the form $\gamma_d \mathcal{D}[a_1^\dagger + a_2]$ between the two QVdP in the dissipative limit, coherences survive in the steady state which leads to entanglement but these are not the ones which follow the selection rule. As we see in fig 6.5, after the critical coupling value of γ_d^E, the oscillators become entangled but the synchronization measure remains zero throughout. This means that the existence of entanglement also doesn't necessarily imply synchronization. Apart from entanglement, even correlations in general don't always mean synchronization. Mutual information is a measure that accounts for all forms of correlations, whether classical or quantum. But even for using this, we have to be careful about where these contributions are coming from, because above all what is important are the selection rule elements. For example, the system of two QVdP coupled via $\gamma_d \mathcal{D}[a_1 + a_2^2]$ also shows an Arnold tongue in mutual information but shows no synchronization at all anywhere in the whole parameter regime.

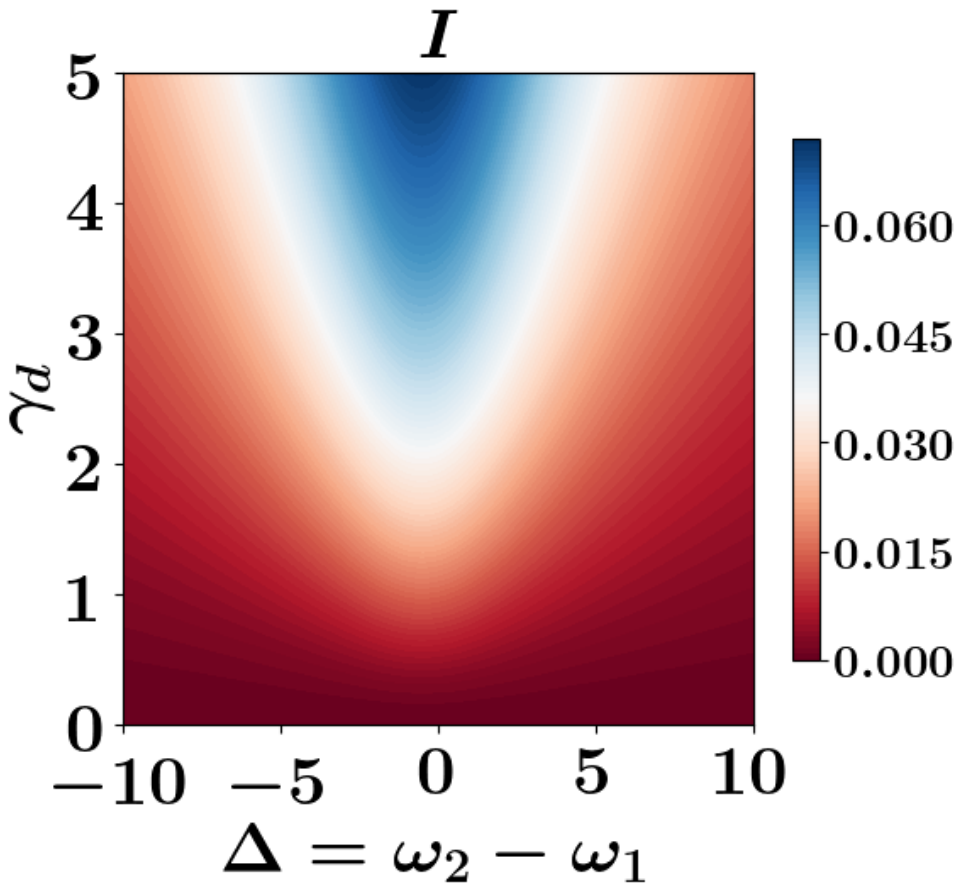

Figure 6.6: Synchronization is a result of specific coherences being present in the system, this sometimes is accompanied by correlations but in general existence of any form of correlation doesn't guarantee synchronization. Here we have two dissipatively coupled QVdP with interaction of the form $\gamma_d \mathcal{D}[a_1 + a_2^2]$ and parameters given by $\gamma_l^{(1)} = \gamma_l^{(2)} = 3$ and $\gamma_g^{(1)} = \gamma_g^{(2)} = 1$, we vary the coupling γ_d from 0 to 5 and detuning Δ from -10 to 10. The system shows an Arnold tongue in mutual information signaling towards the development of correlations but there is no phase locking throughout the parameter regime as could be seen from fig 6.2

Chapter 7

Conclusion

In this thesis, we have explored the synchronization of quantum oscillators, both with an external drive and between two such oscillators. Our study investigated synchronization in self-sustained oscillators modeled using quantum harmonic oscillators (QHO) and spin systems. By analyzing these systems under a unified framework of coherence generation, we provided a broader perspective that integrates previous studies on quantum synchronization.

A key insight from our work is the dependence of synchronization on quantum coherences, which we analyzed using phase-space representations and phase eigenstates $\{|\phi\rangle\}$. We demonstrated that the phase-space distributions for all setups can be expressed as a superposition of harmonic modes $\cos(k\phi)$, with each mode's contribution stemming from a specific subset of coherences S_k. Importantly, we found that synchronization is not solely determined by the magnitude of coherences but also by their relative phases. This suggests the possibility of destructive interference between coherences, which can inhibit synchronization even when coherence norms are high.

For bipartite systems, we established that synchronization is dictated by specific coherences, as determined by selection rules 3.5 and 5.6. This challenges conventional measures of bipartite synchronization, such as the relative entropy of coherence, which considers all forms of coherence indiscriminately. Furthermore, our results clarify the relationship between synchronization and correlations like quantum discord and entanglement. We showed that mutual information and entanglement do not necessarily imply synchronization, clearing up many previous misconceptions in the literature. There exist scenarios where two oscilla-

tors exhibit strong entanglement yet remain unsynchronized, and conversely, synchronized states may exhibit little to no entanglement. These findings highlight the nuanced nature of quantum synchronization and provide a more refined understanding of the role of coherences in this phenomenon. Our results suggest that future research on quantum synchronization should focus not only on quantifying coherence but also on understanding its structural contributions to phase locking.

In conclusion, this work advances the theoretical understanding of quantum synchronization, bridging different approaches under a common framework of coherence generation. It raises important questions about the interplay between coherence, correlations, and synchronization, paving the way for future studies on controlled phase-locking in quantum systems and its potential applications in quantum technologies.

Bibliography

[1] Arkady Pikovsky, Michael Rosenblum, and Jürgen Kurths. Synchronization. *Cambridge university press*, 12, 2001.

[2] Y Kuramoto. Chemical oscillations, waves, and turbulence. *Springer Science and Business Media, 2012*, 8:156, 1984.

[3] Alexander Balanov, Natalia Janson, Dmitry Postnov, and Olga Sosnovtseva. *From simple to complex*. Springer, 2009.

[4] A. Mari, A. Farace, N. Didier, V. Giovannetti, and R. Fazio. Measures of quantum synchronization in continuous variable systems. *Phys. Rev. Lett.*, 111:103605, Sep 2013.

[5] V. Ameri, M. Eghbali-Arani, A. Mari, A. Farace, F. Kheirandish, V. Giovannetti, and R. Fazio. Mutual information as an order parameter for quantum synchronization. *Phys. Rev. A*, 91:012301, Jan 2015.

[6] Livija Cveticanin. On the van der pol oscillator: An overview. *Applied Mechanics and Materials*, 430:3–13, 2013.

[7] Iulia Dumitrescu, Smail Bachir, David Cordeau, Jean-Marie Paillot, and Mihai Iordache. Modeling and characterization of oscillator circuits by van der pol model using parameter estimation. *Journal of Circuits, Systems, and Computers*, 21(05):1250043, 2012.

[8] Kevin Rompala, Richard Rand, and Howard Howland. Dynamics of three coupled van der pol oscillators with application to circadian rhythms. *Communications in Nonlinear Science and Numerical Simulation*, 12(5):794–803, 2007.

[9] Stefan Walter, Andreas Nunnenkamp, and Christoph Bruder. Quantum synchronization of a driven self-sustained oscillator. *Phys. Rev. Lett.*, 112:094102, Mar 2014.

[10] Tony E. Lee and H. R. Sadeghpour. Quantum synchronization of quantum van der pol oscillators with trapped ions. *Phys. Rev. Lett.*, 111:234101, Dec 2013.

[11] Howard J Carmichael. *Statistical methods in quantum optics 1: master equations and Fokker-Planck equations*. Springer Science & Business Media, 2013.

[12] Heinz-Peter Breuer and Francesco Petruccione. *The theory of open quantum systems*. OUP Oxford, 2002.

[13] Thomas L Curtright, David B Fairlie, and Cosmas K Zachos. *A concise treatise on quantum mechanics in phase space*. World Scientific Publishing Company, 2013.

[14] Ulf Leonhardt. *Measuring the quantum state of light*, volume 22. Cambridge university press, 1997.

[15] D. T. Pegg and S. M. Barnett. Phase properties of the quantized single-mode electromagnetic field. *Phys. Rev. A*, 39:1665–1675, Feb 1989.

[16] SM Barnett and DT Pegg. On the hermitian optical phase operator. *Journal of Modern Optics*, 36(1):7–19, 1989.

[17] Leonard Susskind and Jonathan Glogower. Quantum mechanical phase and time operator. *Physics Physique Fizika*, 1:49–61, Jul 1964.

[18] Robert Lynch. The quantum phase problem: a critical review. *Physics Reports*, 256(6):367–436, 1995.

[19] R Barak and Y Ben-Aryeh. Non-orthogonal positive operator valued measure phase distributions of one-and two-modeelectromagnetic fields. *Journal of Optics B: Quantum and Semiclassical Optics*, 7(5):123, 2005.

[20] Michael R. Hush, Weibin Li, Sam Genway, Igor Lesanovsky, and Andrew D. Armour. Spin correlations as a probe of quantum synchronization in trapped-ion phonon lasers. *Phys. Rev. A*, 91:061401, Jun 2015.

[21] C. Davis-Tilley and A. D. Armour. Synchronization of micromasers. *Phys. Rev. A*, 94:063819, Dec 2016.

[22] Niels Lörch, Simon E. Nigg, Andreas Nunnenkamp, Rakesh P. Tiwari, and Christoph Bruder. Quantum synchronization blockade: Energy quantization hinders synchronization of identical oscillators. *Phys. Rev. Lett.*, 118:243602, Jun 2017.

[23] S Swain. Master equation derivation of quantum regression theorem. *Journal of Physics A: Mathematical and General*, 14(10):2577, 1981.

[24] Stefan Walter, Andreas Nunnenkamp, and Christoph Bruder. Quantum synchronization of two van der pol oscillators. *Annalen der Physik*, 527(1-2):131–138, 2015.

[25] Tony E. Lee, Ching-Kit Chan, and Shenshen Wang. Entanglement tongue and quantum synchronization of disordered oscillators. *Phys. Rev. E*, 89:022913, Feb 2014.

[26] A. Luis and L. L. Sánchez-Soto. Probability distributions for the phase difference. *Phys. Rev. A*, 53:495–501, Jan 1996.

[27] F. T. Arecchi, Eric Courtens, Robert Gilmore, and Harry Thomas. Atomic coherent states in quantum optics. *Phys. Rev. A*, 6:2211–2237, Dec 1972.

[28] Kocirc;di HUSIMI. Some formal properties of the density matrix. *Proceedings of the Physico-Mathematical Society of Japan. 3rd Series*, 22(4):264–314, 1940.

[29] X. M. Feng, P. Wang, W. Yang, and G. R. Jin. High-precision evaluation of wigner's d matrix by exact diagonalization. *Phys. Rev. E*, 92:043307, Oct 2015.

[30] Alexandre Roulet and Christoph Bruder. Synchronizing the smallest possible system. *Phys. Rev. Lett.*, 121:053601, Jul 2018.

[31] R. Gilmore, C. M. Bowden, and L. M. Narducci. Classical-quantum correspondence for multilevel systems. *Phys. Rev. A*, 12:1019–1031, Sep 1975.

[32] Cengizhan Ipbüker and I Öztug Bildirici. A general algorithm for the inverse transformation of map projections using jacobian matrices. In *Proceedings of the Third International Symposium Mathematical & Computational Applications*, pages 175–182, 2002.

[33] I Goldhirsch. Phase operator and phase fluctuations of spins. *Journal of Physics A: Mathematical and General*, 13(11):3479, 1980.

[34] Alexandre Roulet and Christoph Bruder. Quantum synchronization and entanglement generation. *Phys. Rev. Lett.*, 121:063601, Aug 2018.

[35] Noufal Jaseem, Michal Hajdušek, Vlatko Vedral, Rosario Fazio, Leong-Chuan Kwek, and Sai Vinjanampathy. Quantum synchronization in nanoscale heat engines. *Phys. Rev. E*, 101:020201, Feb 2020.

[36] Noufal Jaseem, Michal Hajdušek, Parvinder Solanki, Leong-Chuan Kwek, Rosario Fazio, and Sai Vinjanampathy. Generalized measure of quantum synchronization. *Phys. Rev. Res.*, 2:043287, Nov 2020.

[37] V. Ameri, M. Eghbali-Arani, A. Mari, A. Farace, F. Kheirandish, V. Giovannetti, and R. Fazio. Mutual information as an order parameter for quantum synchronization. *Phys. Rev. A*, 91:012301, Jan 2015.

[38] G. Vidal and R. F. Werner. Computable measure of entanglement. *Phys. Rev. A*, 65:032314, Feb 2002.

[39] Harold Ollivier and Wojciech H. Zurek. Quantum discord: A measure of the quantumness of correlations. *Phys. Rev. Lett.*, 88:017901, Dec 2001.

[40] Yichen Huang. Quantum discord for two-qubit x states: Analytical formula with very small worst-case error. *Phys. Rev. A*, 88:014302, Jul 2013.